A young *fibulin-5 +/+*

old *fibulin-5 +/+*

young *fibulin-5 -/-*

B

| | *fibulin-5 +/+* | | *fibulin-5 -/-* | |
| | young | old | young | old |

51 —
39 —

Blot: anti-fibulin-5 Ab

Lane   1 2 3   4 5 6   7 8   9 10

C

FLAG-fibulin-5 / Vector

FLAG-fibulin-5 / Vector

62 —
49 —

Blot: anti-fibulin-5 Ab   anti-FLAG Ab
(BSYN)

D   Full-length fibulin-5

Cleaved fibulin-5

Degradation

▌ FLAG tag   ▭ Ca²⁺-binding EGF-like domain
▌ RGD motif   ▬ Epitope of anti-fibulin-5 Ab (BSYN2473)

Figure 4. **The N-terminal domain cleavage of fibulin-5 is found in aged mouse skin, as well as in cell cultures.** (A) Fine structure of elastic fibers in skin tissues observed by transmission electromicroscopy. Elastin was stained with tannic acid, and therefore appears as black amorphous material. The fine fibers surrounding elastin are microfibrils. Bar, 0.4 μm. (B) Skin tissues were harvested from wild-type or fibulin-5–deficient young (3-mo-old) and old (22-mo-old) mice. Proteins were extracted from skin tissues with 8 M urea and dialyzed against PBS. 10 μg each of these extracts were resolved by SDS-PAGE, and analyzed by Western blotting with anti–fibulin-5 antibody (BSYN2473). Two specific bands of 45 and 55 kD were detected in wild-type mice with anti–fibulin-5 antibody (lanes 1–3). The 55-kD band markedly decreased with age, whereas the 45-kD band markedly increased with age (lanes 4–6). (C) 293T cells were transiently transfected with an expression vector encoding fibulin-5 cDNA with a signal peptide and a FLAG tag at the N terminus. Conditioned medium was subjected to SDS-PAGE, followed by Western blotting analysis with either anti–fibulin-5 or anti-FLAG antibody. Two bands of 55 and 45 kD were detected with anti–fibulin-5 antibody, whereas only a 55-kD band was detected with anti-FLAG antibody. (D) Anti–fibulin-5 antibody (BSYN2473) was raised against a peptide corresponding to amino acids 76–98 (red mark). These findings suggest that fibulin-5 is cleaved at a more N-terminal position than the recognition site of anti–fibulin-5 antibody.

acids 76–98 (Fig. 4 D, red mark). On the other hand, we detected only one 55-kD band with anti-FLAG antibody (Fig. 4 C, right). These results suggest that fibulin-5 may be cleaved at a more N-terminal position than the recognition site of anti–fibulin-5 antibody (Fig. 4 D). We deduced that the lower 45-kD band is the cleaved form of fibulin-5, while the upper 55-kD band is the full-length fibulin-5. The cleaved N-terminal fragment of fibulin-5 appears to be easily degraded because we did not detect a 10-kD band corresponding to this fragment with anti-FLAG antibody.

Fibulin-5 is specifically cleaved after arginine at position 77 by a serine protease

To identify the cleavage site of fibulin-5, we stably transfected the C-terminal–histidine-tagged expression vector encoding fibulin-5 cDNA into 293T cells. We purified recombinant fibulin-5 protein from the conditioned medium of these cells with immobilized metal affinity chromatography, and examined the purified protein by SDS-PAGE. As expected, we detected two bands stained with Coomassie blue, and the lower 45-kD band was assumed to be the cleaved form of fibulin-5. We sequenced the N-terminal end of the lower band using Edman degradation (Fig. 5 A, arrow), and determined that fibulin-5 is cleaved after the arginine at position 77 (Fig. 5 B, top and middle). The upper 55-kD band was also confirmed by protein sequencing to be the full-length fibulin-5, as the N-terminal sequence coincided with the predicted cleavage site after the signal peptide. As many proteases are arginine-specific, we examined whether the

arginine at position 77 is necessary for the cleavage of fibulin-5. We constructed an expression vector encoding R77A mutant fibulin-5, which was mutated from arginine to alanine at position 77 (Fig. 5 B, bottom), and transfected this R77A mutant fibulin-5 vector into 293T cells, followed by Western blotting. As shown in Fig. 5 C, we detected only the upper 55-kD band, whereas the lower 45-kD band disappeared (lane 2), indicating that the R77A mutant fibulin-5 is resistant to cleavage. These results indicate that fibulin-5 is specifically cleaved after the arginine at position 77 (Fig. 5 C, compare lanes 1 and 2), although we cannot rule out the possibility that fibulin-5 might not be cleaved in vivo at the same site as in vitro cell culture. Next, we examined the nature of the protease that cleaves fibulin-5. We transiently transfected the expression vector encoding C-terminal FLAG-tagged fibulin-5 cDNA into 293T cells, and subsequently added different types of protease inhibitors to the culture medium, which was subjected to Western blotting. Whereas a cysteine protease inhibitor, E64, did not inhibit the cleavage of fibulin-5 at all, a serine protease inhibitor, aprotinin, completely inhibited the cleavage (Fig. 5 C, compare lanes 3 and 4). These results indicate that fibulin-5 is cleaved by a serine protease in vitro. We have not yet succeeded in identifying the serine protease that cleaves fibulin-5.

Full-length fibulin-5 can deposit on microfibrils, whereas the truncated form of fibulin-5 cannot

To assess the functional consequence of fibulin-5 cleavage, we studied the interaction of fibulin-5 and microfibrils. Microfibrils,

Figure 5. Fibulin-5 is cleaved after the arginine at position 77 by serine protease and loses the microfibril-associating activity. (A) 293T cells were stably transfected with an expression vector encoding C-terminal-FLAG– and 6× histidine-tagged fibulin-5 cDNA. Recombinant fibulin-5 protein was purified by chelating chromatography from the culture media of these cells, subjected to SDS-PAGE, and stained with Coomassie blue. The lower band (arrow) was subjected to N-terminal sequencing. (B) The N-terminal sequencing of the lower band identified the specific cleavage site of fibulin-5 at the arginine at position 77. (C) 293T cells were transiently transfected with the expression vector encoding C-terminal-FLAG– and 6× histidine-tagged fibulin-5 or R77A mutant fibulin-5, which had a mutation from arginine to alanine at position 77. Transfected cells were cultured for 2 d with or without a cysteine protease inhibitor, E64, or a serine protease inhibitor, aprotinine, added to the culture media. Culture media were then harvested, concentrated by chelating chromatography, and subjected to Western blotting with anti-FLAG antibody. (D–G) Human skin fibroblasts were cultured for 4 d in serum-free medium in the presence of recombinant fibulin-5 (D) or recombinant cleaved fibulin-5 (E) proteins at a concentration of 4 μg/ml in the medium, or without recombinant protein (F). The cells were then double-stained with anti–fibrillin-1 polyclonal antibody (top) and with anti-FLAG monoclonal antibody (middle). Bottom images were produced by superimposition of the top and middle images, together with DAPI nuclear staining. Bars, 60 μm. At the same time, the conditioned medium was immunoblotted with anti-FLAG antibody to confirm that neither fibulin-5 nor cleaved fibulin-5 was degraded during the culture period (G).
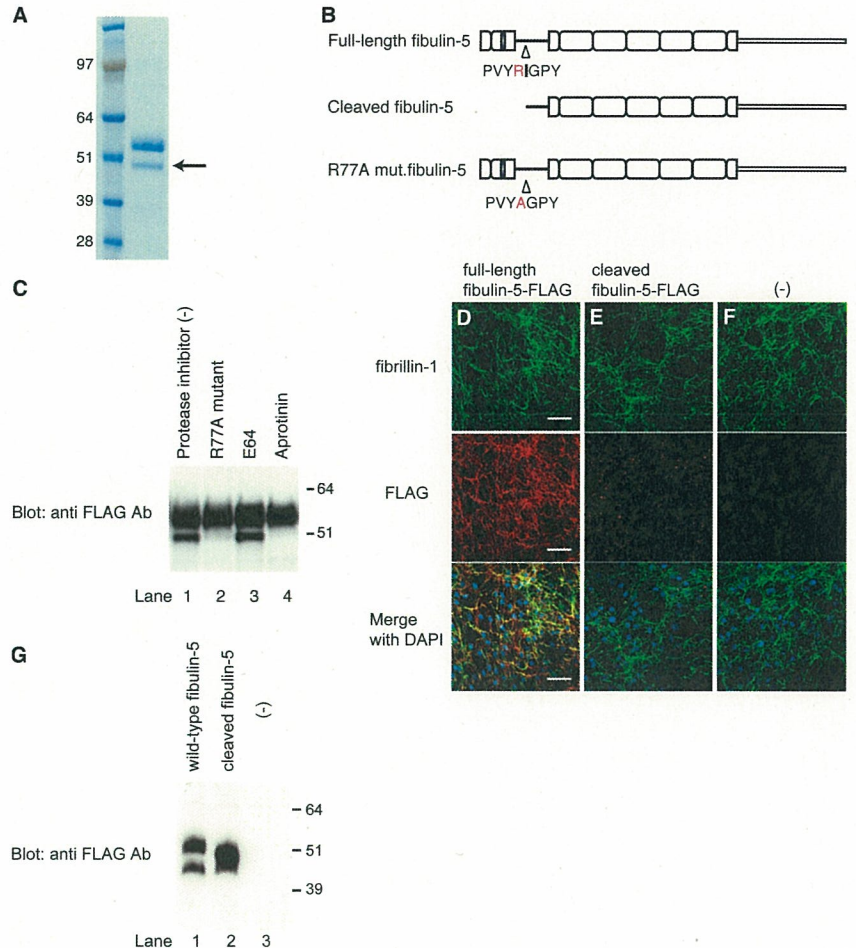
which are mainly composed of fibrillin-1 and -2, are considered to serve as scaffolds for tropoelastin deposition and subsequent elastic fiber assembly. Fibroblast cell cultures developed fine meshworks of fibrillin-1 microfibrils, even under serum-free conditions, at days 4–7 of culture (Fig. 5, D–F); this is much earlier than elastin deposition, which requires >10 d of culture in serum-containing medium. When we added recombinant fibulin-5 protein to the culture, fibulin-5 colocalized with fibrillin-1 microfibrils. However, when we added recombinant truncated fibulin-5 protein to the culture, the added truncated fibulin-5 did not deposit on fibrillin-1 microfibrils. This was not because the truncated form of fibulin-5 is susceptible to degradation, as Western blot analysis of the culture medium showed that truncated form of fibulin-5 was as stable as the full-length fibulin-5 in the medium (Fig. 5 G). These data indicate that full-length fibulin-5 can deposit on microfibrils, whereas the truncated form of fibulin-5 cannot.

The cleavage of fibulin-5 causes inactivation of the elastogenic activity of fibulin-5

Next, we investigated the consequences of the functional change caused by the cleavage of fibulin-5 in elastic fiber assembly, using the in vitro elastogenesis assay shown in Fig. 1 A with recombinant fibulin-5 and the truncated form of fibulin-5 proteins. Whereas wild-type fibulin-5 potently induced elastic fiber development, the truncated form of fibulin-5 did not induce elastic

fiber development at all (Fig. 6, B and C). Therefore, we concluded that the cleavage of fibulin-5 causes inactivation of the elastogenic activity of fibulin-5.

Cross-linking of elastin is promoted by prealigned fibulin-5 on microfibrils

The assembly of functional elastic fibers requires not only fibrillar deposition and coacervation of tropoelastin, but also cross-linking of tropoelastin. The aforementioned data suggest that deposition of fibulin-5 onto microfibrils accelerates fibrillar tropoelastin deposition, but it was not clear if the tropoelastin molecules are cross-linked to form mature functional elastic fibers. To examine this, we added β-aminopropionitrile (BAPN), an irreversible inhibitor of LOXs (Tang et al., 1983), to serum-free skin fibroblast culture containing recombinant fibulin-5 protein. It is known that LOXs, which are cross-linking enzymes for elastin monomers, are necessary for elastic fiber maturation (Hornstra et al., 2003; Liu et al., 2004; Maki et al., 2002). As shown in Fig. 6 D, elastins showed only a dotlike deposition when elastin cross-linking was largely inhibited by BAPN, whereas fibrillar deposition of fibulin-5 on microfibrils was not affected by BAPN. This punctuate distribution of elastin is displayed by tropoelastin coacervates before cross-linking (Clarke et al., 2006). These data indicate that elastic fibers organized by the addition of fibulin-5 protein are cross-linked and mature fibers, and that not only deposition and aggregation but also
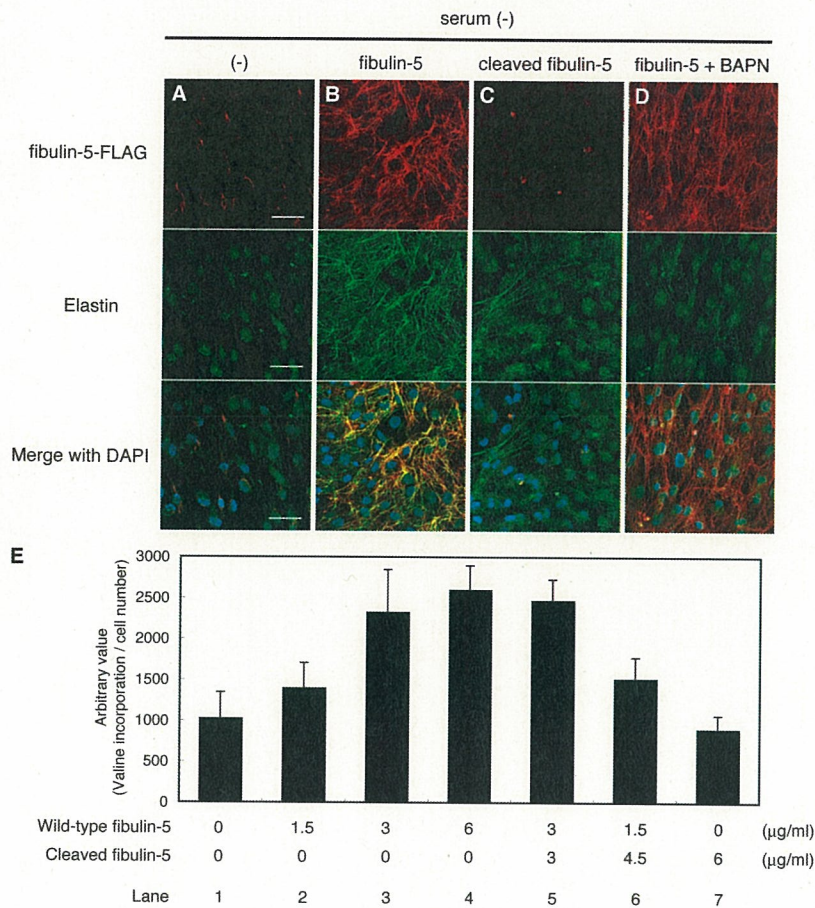
Figure 6. **Fibulin-5 loses its elastogenic activity upon proteolytic cleavage.** (A–E) Human skin fibroblasts were cultured in serum-free media without addition of proteins (A), with wild-type fibulin-5 (B), with the cleaved form of fibulin-5 (C), or with wild-type fibulin-5 and 500 μM BAPN (D). Each FLAG-tagged recombinant protein was added to the culture at a final concentration of 4 μg/ml. Cultures were stained with anti-FLAG antibody (top) and anti–human elastin antibody (middle). The bottom images were produced by superimposition of the top and middle images, together with DAPI nuclear staining. Bars, 50 μm. (E) Quantitation of insoluble (i.e., cross-linked and mature) elastin produced by cells cultured with various amounts of wild-type and cleaved fibulin-5 added to the medium. Cultured skin fibroblasts were metabolically labeled with [^{3}H]valine during the culture period, and the radioactivity of the NaOH-insoluble fractions was quantitated. The radioactivity count was corrected by the relative cell number of separate wells measured with a modified MTT assay, although neither wild-type nor cleaved fibulin-5 significantly affected the cell number (not depicted). Data were obtained as quadruplicates, and the mean ± the SD is shown.

cross-linking of elastin is promoted by prealigned fibulin-5 on microfibrils.

The N-terminal domain-truncated fibulin-5 loses the elastogenic activity, but does not interfere with elastic fiber assembly

We next examined whether cleaved fibulin-5 is merely inactive or works against elastogenesis in a dominant-negative manner. For this purpose, we quantified the amount of elastic fibers induced by full-length fibulin-5 with or without cleaved fibulin-5. We metabolically labeled newly synthesized elastin with [^{3}H]valine (Keeley, 1976), and measured the incorporation of [^{3}H]valine in the NaOH-insoluble fraction of these cells, which reflects the amount of mature elastic fibers (Hinek et al., 2000). As shown in Fig. 6 E, we detected substantial, dose-dependent incorporation of [^{3}H]valine upon adding recombinant fibulin-5 to the medium (Fig. 6 E, compare lanes 1–4). On the other hand, cleaved fibulin-5 showed neither an additive nor a dominant-negative effect on fibulin-5–induced elastic fiber development (Fig. 6 E, compare lanes 1–7). These results indicate that fibulin-5 simply loses its elastogenic activity as a result of cleavage of the N-terminal domain.

LOXL1, 2, and 4 proteins mainly interact with the C-terminal domain of fibulin-5

To develop mature elastic fibers, tropoelastin molecules need to be highly cross-linked by LOXs. Five LOX family members

have been identified so far, LOX, LOXL1, 2, 3, and 4 (Molnar et al., 2003). Mice lacking LOX and mice lacking LOXL1 were recently reported to show profound fragmentation of elastic fibers (Maki et al., 2002; Hornstra et al., 2003; Liu et al., 2004). Moreover, LOXL1 has been reported to interact with fibulin-5 (Liu et al., 2004). To investigate whether fibulin-5 interacts with other LOX family members, we performed in vitro binding assays using Myc-tagged LOX and LOXLs, and the set of FLAG-tagged fibulin-5 deletion mutant constructs shown in Fig. 7 A. As shown in Fig. 7 B, we detected the specific interaction of LOXL1, 2, and 4 proteins with fibulin-5 protein (top, lanes 1, 7, and 13). The interaction of fibulin-5 and these LOXL proteins was eliminated or considerably diminished by the C-terminal deletion of fibulin-5 (Fig. 7 B, top, lanes 5, 11, and 17). These results indicate that LOXL1, 2, and 4 proteins mainly interact with the C-terminal domain of fibulin-5. We also detected substantial, but weak, interaction of fibulin-5 with LOX and LOXL3 in in vitro binding assays (unpublished data). However, we could not determine the specificity of these interactions because all of the fibulin-5 deletion mutants tested seemed to weakly interact with LOX or LOXL3. Intriguingly, the fibulin-5–LOXL1 interaction was markedly diminished by N-terminal deletion of fibulin-5 (Fig. 7 B, top left, lanes 2 and 3). Thus, fibulin-5 does not interact with LOXL1 after cleavage of fibulin-5, and this defect might contribute to the loss of elastogenic activity.

Figure 7. Fibulin-5 interacts with LOXL enzymes. (A) Domain structures of the full-length fibulin-5 and the fibulin-5 deletion mutants used for in vitro binding assays. ΔN1-fibulin-5 corresponds to the naturally cleaved form of fibulin-5. These mutants were expressed as C-terminal-FLAG–tagged proteins. (B) Fibulin-5 binds to LOXL1, 2, and 4 through the C-terminal domain. 293T cells were transiently transfected with the vectors shown in A or a mock vector. Expression vectors for Myc-tagged LOX or LOXLs were also independently transfected into 293T cells. The conditioned media were harvested, and mixed. Each mixture was subjected to immunoprecipitation with anti-FLAG antibody, separated by SDS-PAGE, and analyzed by Western blotting with a monoclonal anti-Myc antibody.
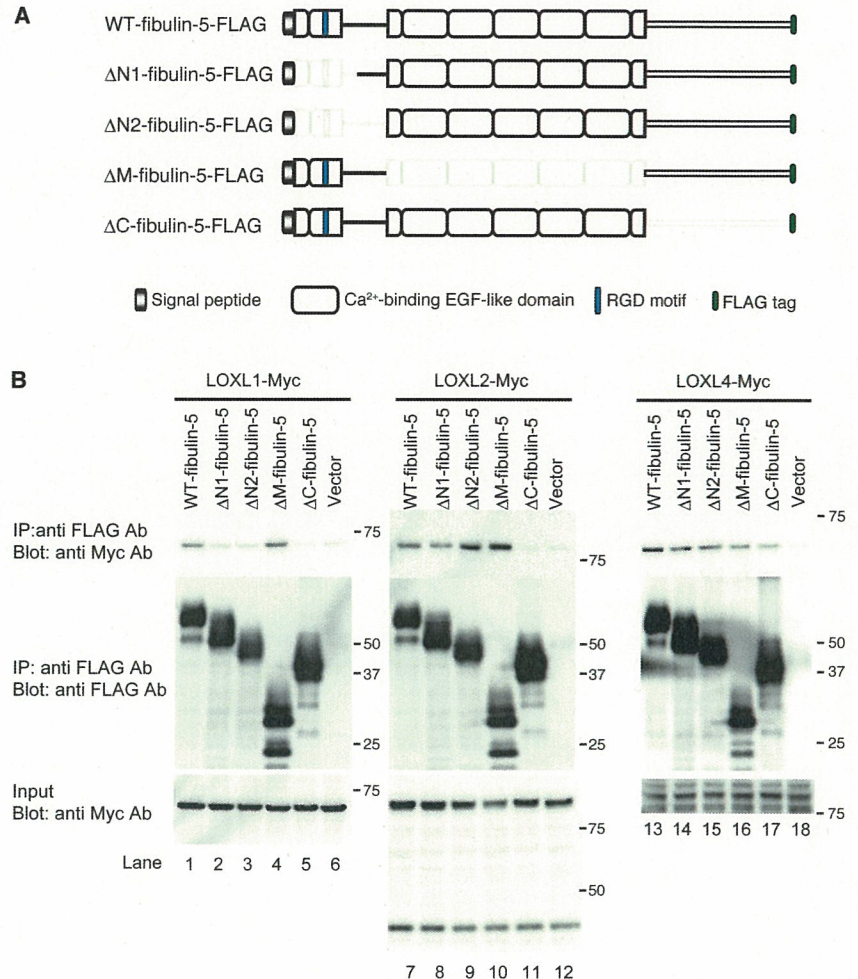
Discussion

We have identified an elastic fiber–organizing activity of fibulin-5/DANCE protein that is abrogated by proteolytic cleavage of the N-terminal domain in cell culture and in vivo. Our proposed molecular mechanism of elastic fiber organization by fibulin-5/DANCE protein is illustrated in Fig. 8 A. We call this the "Line DANCE model." According to this model, full-length fibulin-5 protein associates with microfibrils. Direct interaction of fibulin-5 and fibrillin-1 (Freeman et al., 2005) may be important for this association. As fibulin-5 serves as an integrin ligand through its N-terminal domain (Nakamura et al., 1999, 2002), integrin–fibulin-5 interaction, in addition to integrin–fibrillin interaction, may help the assembly to occur in the proximity of the cell surface. After fibulin-5 interacts with microfibrils, tropoelastins accumulate on fibulin-5 proteins and coacervate. LOXL enzymes tethered on the C-terminal domain of fibulin-5 promote cross-linking of the aggregated tropoelastins, to form mature elastic fibers. In contrast, as illustrated in Fig. 8 B, the truncated form of fibulin-5 cannot associate with microfibrils or integrins, and therefore is unable to promote the organization of the elastic fiber assembly, although the truncated form of fibulin-5 itself has the ability to bind tropoelastin and enhance coacervation of tropoelastin as well (unpublished data).

In this study, we first succeeded in inducing the development of elastic fibers in serum-free skin fibroblast culture by adding purified fibulin-5 protein. Tropoelastin and other elastic fiber components were not organized into elastic fibers without addition of fibulin-5 protein, suggesting that fibulin-5 is not only a necessary component of elastic fibers (Nakamura et al., 2002; Yanagisawa et al., 2002) but also an organizer that can induce elastic fiber assembly. Skin fibroblasts are known to develop abundant elastic fibers in serum-containing media. However, serum contains various known and unknown factors, such as cytokines and growth factors, and also causes increases of total cell number and cell density, making it difficult to identify specific molecules that are important for elastogenesis. Indeed, we detected a significant amount of fibulin-5 in serum using immunoprecipitation and ELISA (unpublished data), which might contribute to the elastogenic activity of the serum to some extent. We detected abundant deposition of fibulin-5 that may be derived from fibroblasts or from serum in serum-containing culture of skin fibroblasts, whereas endogenous fibulin-5 was scarcely detected in serum-free culture (Fig. S1). This indicates that the dose of fibulin-5 is crucial for elastic fiber organization in this serum-free cell culture, and that the endogenous expression of fibulin-5 alone is insufficient. Our serum-free elastogenesis system, in combination with gene knockdown by RNAi, would
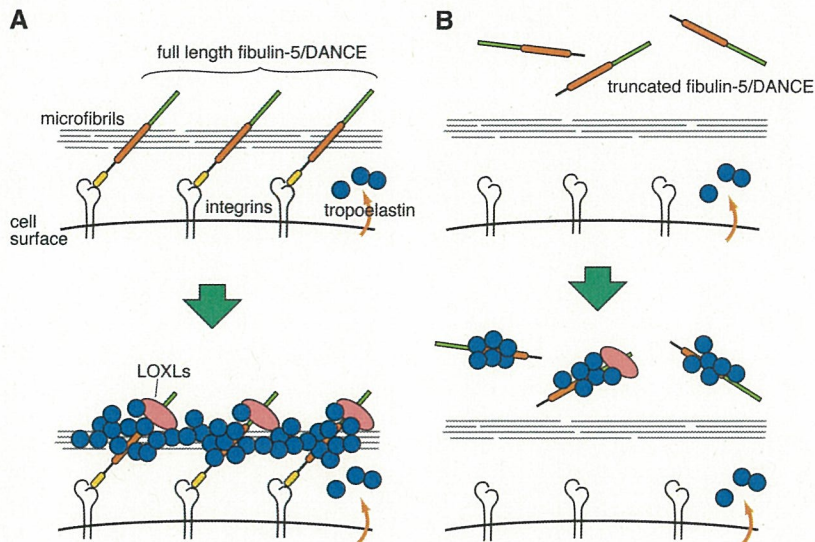
Figure 8. **The Line DANCE model.** (A) This model illustrates how fibulin-5/DANCE promotes fibrillar deposition and cross-linking of tropoelastin molecules on microfibrils to promote the development of mature elastic fibers. (B) Truncated fibulin-5 cannot be deposited on microfibrils, and therefore cannot promote elastic fiber assembly.

be a useful tool to identify other factors that regulate elastic fiber assembly, as unknown factors in the serum need not be taken into account.

It has been reported that fibulin-5 can strongly interact with tropoelastin (Yanagisawa et al., 2002). We found that fibulin-5 not only binds with tropoelastin, but also promotes co-acervation of tropoelastins, and thus plays a more positive role in the alignment and deposition of tropoelastin. Fibrillin-1 has also recently been reported to promote coacervation (Clarke et al., 2005). Because fibulin-5 interacts with both fibrillin-1 and tropoelastins (Yanagisawa et al., 2002; Freeman et al., 2005), a fibulin-5–fibrillin-1 complex might cooperatively promote coacervation. Coacervated tropoelastin molecules need to be cross-linked by LOX family enzymes for the development of mature elastic fibers. Our data show that fibulin-5 also promotes cross-linking of tropoelastin, which may be mediated by recruiting LOXL1, 2, and 4 in the vicinity of coacervated tropoelastin (Fig. 7 B).

We found that a much higher level of the truncated form of fibulin-5 was present in aged mouse skin than in young mouse skin (Fig. 4 B). There are several possible interpretations of this result: (a) fibulin-5 might be cleaved because of more protease activity in aged tissues; (b) truncated fibulin-5 might be stable and accumulate during life; or (c) truncated fibulin-5 might be more easily extracted from aged elastic fibers than from young elastic fibers. In any case, the truncated form of fibulin-5 cannot contribute to new elastogenesis, and therefore the decrease in full-length fibulin-5 may directly reflect a decrease in the elastogenic activity of aged tissues.

In this study, we could not exclude the possibility that the truncated form of fibulin-5 might play some roles in elasto-genesis in vivo. Although truncated fibulin-5 cannot contribute to new elastogenesis as it cannot interact with microfibrils, fibulin-5 protein cleaved after deposition onto microfibrils might take part in subsequent processes of elastogenesis, as binding with tro-poelastin and facilitating coacervation of tropoelastin are not compromised by the N-terminal domain cleavage (unpublished data).

To clarify the physiological consequences of the cleavage of fibulin-5, further studies will be needed using gene-targeted mice in which a cleavage-resistant mutant form of fibulin-5 is knocked-in.

So far, elastic matrices have been considered to be designed to maintain elastic function for a lifetime (Kielty et al., 2002). Elastin is reported to have an exceptionally long half-life, and to have a turnover rate which approaches our lifespan (Shapiro et al., 1991). On the other hand, elastase activity is provoked by exposure to sunlight and by smoking, causing degradation of the elastic fibers of the skin and lung, respectively (Fisher et al., 1996; Hautamaki et al., 1997). This implies that elastogenic activity needs to be maintained even in the adult tissues to regenerate elastic fibers. Indeed, we detected a significant amount of fibulin-5 in the serum of aged mice (unpublished data), and we and others reported that the expression of fibulin-5 is up-regulated in some path-ological conditions, such as in atherosclerotic lesions (Kowal et al., 1999; Nakamura et al., 1999; Nguyen et al., 2004), lung injury by elastase (Kuang et al., 2003), and pulmonary hypertension (Merklinger et al., 2005). The potent elasto-genic activity of fibulin-5 might provide future therapeutic applications for aging-associated diseases, such as emphy-sema and arteriosclerosis, or cosmetic applications for wrinkled skin. Application of fibulin-5 might be extended to tissue engineering, to make elastic skin or vessels by using cell cultures. Further studies are needed to examine whether fibulin-5 might improve age-related changes of elastic ma-trices in vivo.

In summary, we demonstrated the elastic fiber organizing activity of fibulin-5 that is abrogated by age-associated pro-teolytic cleavage. We demonstrated that the addition of recom-binant fibulin-5 protein induces elastic fiber development, and that a decrease in full-length fibulin-5 caused by proteolytic cleavage may contribute to the loss of the elastogenic potential in aged elastic tissues. Our findings might provide a molecular pathway to future therapeutic applications of the elastic fiber organizing activity of fibulin-5.

Materials and methods

Cell culture
293T cells and human skin fibroblasts (HSFs) were maintained in DME (Sigma-Aldrich) supplemented with 2 mM glutamine, 10% penicillin/streptomycin, and 10% FBS at 37°C in 5% CO_2. HSFs were provided by M. Naito (Kyoto University, Kyoto, Japan).

Plasmid construction
Human full-length fibulin-5 cDNA was cloned as previously described (Nakamura et al., 1999). pEF6/V5 (Invitrogen) was modified by incorporation of a C-terminal FLAG-tag or Myc-tag (pEF6/FLAG, pEF6/Myc). The fibulin-5 ΔN1- (Δnt 247–399), ΔN2- (Δnt 247–504), ΔM- (Δnt 505–1,110), and ΔC- (Δnt 1, 114–1,512) fibulin-5 cDNAs were subcloned into pEF6/FLAG. Human fibulin-5 cDNA sequences are numbered according to GenBank accession no. AF112152. Human full-length LOXL1, 2, 3, and 4 cDNAs were obtained from IMAGE (available from GenBank under accession no. BC015090, BC000594, BC071865, and BC013153, respectively), and subcloned into pEF6/Myc. All constructs were confirmed by sequencing (ABI Prism 3100).

Protein purification
pEF6/V5 (Invitrogen) was modified by incorporation of a C-terminal histidine and FLAG-tag. Human wild-type and each mutant fibulin-5 cDNA were subcloned into pEF6/FLAG-His. The respective stable blasticidin-resistant 293T cell clones were then obtained by transfection with these expression vectors. Recombinant proteins were purified from the serum-free conditioned medium of stable lines using Ni-NTA metal affinity resin (QIAGEN), and desalted with a Hi-Trap desalting column (GE Healthcare). Protein concentrations were determined with Coomassie Plus-200 Protein Assay Reagent (Pierce Chemical Co.). Human tropoelastin cDNA was cloned from human skin fibroblasts by RT-PCR. Of the four splice variants obtained, the longest cDNA, which codes one of the splicing variants of the elastin gene (ELNc; available from GenBank under accession no. BC035570), was subcloned into pTrcHis vector (Invitrogen) and expressed in bacteria, followed by protein purification with Ni-NTA column (GE Healthcare), as previously described (Wachi et al., 2005).

In vitro elastogenesis assay and immunofluorescence
HSFs were subconfluently plated on microscope cover glasses (Fisher Scientific). 3 d after plating, culture media were changed to serum-free DME/F12 (Sigma-Aldrich), and purified recombinant fibulin-5 proteins were added, and the incubation was continued for another 10 d. The cells were fixed with 100% methanol, and blocked with 2% BSA. The primary antibodies used were anti-FLAG M2 monoclonal (1/100; Sigma-Aldrich), anti–human elastin polyclonal (1/100; EPC, PR533), anti–human fibulin-5 monoclonal (1/100; 10A), and anti–human fibrillin-1 polyclonal (1/100; EPC, PR217) antibodies. The secondary antibodies used were Alexa Fluor 488, 546, or 647 anti–rabbit or –mouse IgG (1/100; Invitrogen). After staining with DAPI, stained cells were mounted with a Prolong Gold Antifade Kit (Invitrogen). Fluorescence images were sequentially collected using a confocal microscope featuring 405-, 488-, 543-, and 633-nm laser lines with an open pinhole setting operated by the built-in software; either a microscope (LSM510 META; Carl Zeiss MicroImaging, Inc.) with a C-Apo 40×/1.2 NA lens (Figs. 1 and 6) or a microscope (FV-1000; Olympus) with a UPlanSApo 40×/0.9 NA lens (Figs. 5 and S1). Image files were converted to TIFF format using the operating software, merged, linearly contrast stretched (with the same setting in each set of experiments) using Photoshop CS2 (Adobe), and imported into Illustrator CS2 (Adobe) for assembly. Anti–human fibulin-5 monoclonal antibody (10A) was raised by Iwaki Co., Ltd. by immunization of fibulin-5–deficient mice with purified recombinant human fibulin-5 protein.

Coacervation assay
Coacervation of tropoelastin with or without fibulin-5 protein was assessed using the method described (Clarke et al., 2005). Soluble tropoelastin and fibulin-5 were prepared in PBS and mixed on ice. Each reaction mixture was transferred to an 8-channel quartz cuvette for light scattering measurements at 440 nm. The temperature of a spectrophotometer (UV-1650; Shimazu) fitted with a heating/cooling block was regulated by a circulating water bath. All channels were simultaneously cooled and heated in the heating/cooling block by the circulating water.

Transfection, in vitro binding assay, and Western blotting
293T cells were transfected using Lipofectamine PLUS (Invitrogen). The mixtures of conditioned media were subjected to immunoprecipitation with anti-FLAG M2 affinity gel (Sigma-Aldrich). After washing, immune complexes were resolved by SDS-PAGE, transferred to PVDF membranes (Bio-Rad Laboratories), and reacted with HRP-conjugated anti-Myc monoclonal (9E10; 1/500; Santa Cruz Biotechnology) or anti-FLAG M2 monoclonal (1/1,000; Sigma-Aldrich) antibody. Signals were detected using Western Lightning Chemiluminescence Reagent PLUS (Perkin Elmer).

Tissue extraction and Western blotting
Proteins were extensively extracted from skin tissues with 8 M urea solution. After dialysis against PBS, the protein concentration was measured with Coomassie Plus-200 Protein Assay Reagent. Protein samples of the same amount were subjected to SDS-PAGE (Invitrogen), followed by Western blotting with anti–fibulin-5 antibody (1/400, BSYN2473). HRP-conjugated anti–rabbit antibody (1/2,000; Santa Cruz Biotechnology) was used as a secondary antibody.

Transmission electron microscopy
For transmission electron microscopy, skin tissues were fixed with 4% paraformaldehyde, 2.5% glutaraldehyde, 0.1% tannic acid in 0.1 M cacodylate buffer. Sections were then stained with uranyl acetate.

Quantitative measurement of insoluble elastin
HSFs were subconfluently plated on 60-mm dishes in quadruplicates. 3 d after plating, 20 μCi [^{3}H]valine was added to each dish, together with purified recombinant fibulin-5 protein or cleaved fibulin-5 protein. The cultures were then incubated at 37°C in 5% CO_2 for 10 d. The cells were harvested in 0.1 M acetic acid on ice. After centrifugation, the pellets were boiled in 0.1 N NaOH for 1 h. Subsequently, the NaOH-insoluble pellets were boiled with 5.7 N HCl for 1 h, mixed with scintillation fluid, and measured for radioactivity with a scintillation counter (Beckman Coulter).

Reverse transcription-polymerase chain reaction and quantitative PCR
Total RNAs were extracted using RNeasy Plus Mini Kit (QIAGEN) and transcribed to cDNA with random hexamers using the SuperScript III First-Strand Synthesis System (Invitrogen). For quantitative PCR, the reaction was performed with a QuantiTect SYBR Green PCR kit (QIAGEN), and the products were analyzed with the Mx3000P QPCR System (Stratagene). Primers used for quantitative PCR are provided in Table S1 (available at http://www.jcb.org/cgi/content/full/jcb.200611026/DC1).

Online supplemental material
Fig. S1 shows that serum induces fibulin-5 deposition on microfibrils. Table S1 shows primers used for quantitative PCR. The online version of this article is available at http://www.jcb.org/cgi/content/full/jcb.200611026/DC1.

References

Bailey, A.J. 2001. Molecular mechanisms of ageing in connective tissues. *Mech. Ageing Dev.* 122:735–755.

Carta, L., L. Pereira, E. Arteaga-Solis, S.Y. Lee-Arteaga, B. Lenart, B. Starcher, C.A. Merkel, M. Sukoyan, A. Kerkis, N. Hazeki, et al. 2006. Fibrillins 1 and 2 perform partially overlapping functions during aortic development. *J. Biol. Chem.* 281:8016–8023.

Clarke, A.W., S.G. Wise, S.A. Cain, C.M. Kielty, and A.S. Weiss. 2005. Coacervation is promoted by molecular interactions between the PF2 segment of fibrillin-1 and the domain 4 region of tropoelastin. *Biochemistry.* 44:10271–10281.

Clarke, A.W., E.C. Arnspang, S.M. Mithieux, E. Korkmaz, F. Braet, and A.S. Weiss. 2006. Tropoelastin massively associates during coacervation to form quantized protein spheres. *Biochemistry.* 45:9989–9996.

Fisher, G.J., S.C. Datta, H.S. Talwar, Z.Q. Wang, J. Varani, S. Kang, and J.J. Voorhees. 1996. Molecular basis of sun-induced premature skin ageing and retinoid antagonism. *Nature.* 379:335–339.

Freeman, L.J., A. Lomas, N. Hodson, M.J. Sherratt, K.T. Mellody, A.S. Weiss, A. Shuttleworth, and C.M. Kielty. 2005. Fibulin-5 interacts with fibrillin-1 molecules and microfibrils. *Biochem. J.* 388:1–5.

Hautamaki, R.D., D.K. Kobayashi, R.M. Senior, and S.D. Shapiro. 1997. Requirement for macrophage elastase for cigarette smoke-induced emphysema in mice. *Science.* 277:2002–2004.

Hinek, A., A.C. Smith, E.M. Cutiongco, J.W. Callahan, K.W. Gripp, and R. Weksberg. 2000. Decreased elastin deposition and high proliferation of fibroblasts from Costello syndrome are related to functional deficiency in the 67-kD elastin-binding protein. *Am. J. Hum. Genet.* 66:859–872.

Hornstra, I.K., S. Birge, B. Starcher, A.J. Bailey, R.P. Mecham, and S.D. Shapiro. 2003. Lysyl oxidase is required for vascular and diaphragmatic development in mice. *J. Biol. Chem.* 278:14387–14393.

Kagan, H.M., and W. Li. 2003. Lysyl oxidase: properties, specificity, and biological roles inside and outside of the cell. *J. Cell. Biochem.* 88:660–672.

Keeley, F.W. 1976. A convenient method for the identification and estimation of soluble elastin synthesis in vitro. *Connect. Tissue Res.* 4:193–203.

Kielty, C.M., M.J. Sherratt, and C.A. Shuttleworth. 2002. Elastic fibres. *J. Cell Sci.* 115:2817–2828.

Kowal, R.C., J.A. Richardson, J.M. Miano, and E.N. Olson. 1999. EVEC, a novel epidermal growth factor-like repeat-containing protein upregulated in embryonic and diseased adult vasculature. *Circ. Res.* 84:1166–1176.

Kuang, P.P., R.H. Goldstein, Y. Liu, D.C. Rishikof, J.C. Jean, and M. Joyce-Brady. 2003. Coordinate expression of fibulin-5/DANCE and elastin during lung injury repair. *Am. J. Physiol. Lung Cell. Mol. Physiol.* 285:L1147–L1152.

Liu, X., Y. Zhao, J. Gao, B. Pawlyk, B. Starcher, J.A. Spencer, H. Yanagisawa, J. Zuo, and T. Li. 2004. Elastic fiber homeostasis requires lysyl oxidase-like 1 protein. *Nat. Genet.* 36:178–182.

Maki, J.M., J. Rasanen, H. Tikkanen, R. Sormunen, K. Makikallio, K.I. Kivirikko, and R. Soininen. 2002. Inactivation of the lysyl oxidase gene Lox leads to aortic aneurysms, cardiovascular dysfunction, and perinatal death in mice. *Circulation.* 106:2503–2509.

Mecham, R.P. 1987. Modulation of elastin synthesis: in vitro models. *Methods Enzymol.* 144:232–246.

Merklinger, S.L., R.A. Wagner, E. Spiekerkoetter, A. Hinek, R.H. Knutsen, M.G. Kabir, K. Desai, S. Hacker, L. Wang, G.M. Cann, et al. 2005. Increased fibulin-5 and elastin in S100A4/Mts1 mice with pulmonary hypertension. *Circ. Res.* 97:596–604.

Molnar, J., K.S. Fong, Q.P. He, K. Hayashi, Y. Kim, S.F. Fong, B. Fogelgren, K.M. Szauter, M. Mink, and K. Csiszar. 2003. Structural and functional diversity of lysyl oxidase and the LOX-like proteins. *Biochim. Biophys. Acta.* 1647:220–224.

Nakamura, T., P. Ruiz-Lozano, V. Lindner, D. Yabe, M. Taniwaki, Y. Furukawa, K. Kobuke, K. Tashiro, Z. Lu, N.L. Andon, et al. 1999. DANCE, a novel secreted RGD protein expressed in developing, atherosclerotic, and balloon-injured arteries. *J. Biol. Chem.* 274:22476–22483.

Nakamura, T., P.R. Lozano, Y. Ikeda, Y. Iwanaga, A. Hinek, S. Minamisawa, C.F. Cheng, K. Kobuke, N. Dalton, Y. Takada, et al. 2002. Fibulin-5/DANCE is essential for elastogenesis in vivo. *Nature.* 415:171–175.

Nguyen, A.D., S. Itoh, V. Jeney, H. Yanagisawa, M. Fujimoto, M. Ushio-Fukai, and T. Fukai. 2004. Fibulin-5 is a novel binding protein for extracellular superoxide dismutase. *Circ. Res.* 95:1067–1074.

Pasquali-Ronchetti, I., and M. Baccarani-Contri. 1997. Elastic fiber during development and aging. *Microsc. Res. Tech.* 38:428–435.

Rosenbloom, J., W.R. Abrams, and R. Mecham. 1993. Extracellular matrix 4: the elastic fiber. *FASEB J.* 7:1208–1218.

Shapiro, S.D., S.K. Endicott, M.A. Province, J.A. Pierce, and E.J. Campbell. 1991. Marked longevity of human lung parenchymal elastic fibers deduced from prevalence of D-aspartate and nuclear weapons-related radiocarbon. *J. Clin. Invest.* 87:1828–1834.

Tang, S.S., P.C. Trackman, and H.M. Kagan. 1983. Reaction of aortic lysyl oxidase with beta-aminopropionitrile. *J. Biol. Chem.* 258:4331–4338.

Urry, D.W. 1988. Entropic elastic processes in protein mechanisms. I. Elastic structure due to an inverse temperature transition and elasticity due to internal chain dynamics. *J. Protein Chem.* 7:1–34.

Vrhovski, B., S. Jensen, and A.S. Weiss. 1997. Coacervation characteristics of recombinant human tropoelastin. *Eur. J. Biochem.* 250:92–98.

Wachi, H., F. Sato, H. Murata, J. Nakazawa, B.C. Starcher, and Y. Seyama. 2005. Development of a new in vitro model of elastic fiber assembly in human pigmented epithelial cells. *Clin. Biochem.* 38:643–653.

Yanagisawa, H., E.C. Davis, B.C. Starcher, T. Ouchi, M. Yanagisawa, J.A. Richardson, and E.N. Olson. 2002. Fibulin-5 is an elastin-binding protein essential for elastic fibre development in vivo. *Nature.* 415:168–171.

Zanetti, M., P. Braghetta, P. Sabatelli, I. Mura, R. Doliana, A. Colombatti, D. Volpin, P. Bonaldo, and G.M. Bressan. 2004. EMILIN-1 deficiency induces elastogenesis and vascular cell defects. *Mol. Cell. Biol.* 24:638–650.

RESEARCH ARTICLE

Reduced Secretion of Fibulin 5 in Age-Related Macular Degeneration and Cutis Laxa

Andrew J. Lotery,[1,2]* Dominique Baas,[3] Caroline Ridley,[4] Richard P.O. Jones,[4,9] Caroline C.W. Klaver,[5] Edwin Stone,[6] Tomoyuki Nakamura,[7] Andrew Luff,[2] Helen Griffiths,[1] Tao Wang,[4,9] Arthur A.B. Bergen,[3,8] and Dorothy Trump[4]

[1]Human Genetics Division, University of Southampton, Southampton, Hampshire, United Kingdom; [2]Southampton Eye Unit, Southampton University Hospital Trust, Southampton, Hampshire, United Kingdom; [3]Department of Clinical and Molecular Ophthalmogenetics, The Netherlands Ophthalmic Research Institute, Amsterdam, The Netherlands; [4]Academic Unit of Medical Genetics, School of Medicine, University of Manchester, Manchester, United Kingdom; [5]Department of Ophthalmology, Erasmus Medical Center, Rotterdam, Rotterdam, The Netherlands; [6]Center for Macular Degeneration, University of Iowa Hospitals and Clinics, Iowa City, Iowa; [7]Horizontal Medical Research Organization, Cardiovascular Development Unit, Kyoto University School of Medicine, Kyoto, Japan; [8]Department of Clinical Genetics, Academic Medical Center, Amsterdam, Amsterdam, The Netherlands; [9]Centre for Molecular Medicine, Faculty of Medical and Health Sciences, University of Manchester, Manchester, United Kingdom

Communicated by Daniel F. Schorderet

Age-related macular degeneration (ARMD) is the leading cause of irreversible visual loss in the Western world, affecting approximately 25 million people worldwide. The pathogenesis is complex and missense mutations in FBLN5 have been reported in association with ARMD. We have investigated the role of fibulin 5 in ARMD by completing the first European study of the gene FBLN5 in ARMD (using 2 European cohorts of 805 ARMD patients and 279 controls) and by determining the functional effects of the missense mutations on fibulin 5 expression. We also correlated the FBLN5 genotype with the ARMD phenotype. We found two novel sequence changes in ARMD patients that were absent in controls and expressed these and the other nine reported FBLN5 mutations associated with ARMD and two associated with the autosomal recessive disease cutis laxa. Fibulin 5 secretion was significantly reduced ($P < 0.001$) for four ARMD (p.G412E, p.G267S, p.I169T, and p.Q124P) and two cutis laxa (p.S227P, p.C217R) mutations. These results suggest that some missense mutations associated with ARMD lead to decreased fibulin 5 secretion with a possible corresponding reduction in elastinogenesis. This study confirms the previous work identifying an association between FBLN5 mutations and ARMD and for the first time suggests a functional mechanism by which these mutations can lead to ARMD. It further demonstrates that FBLN5 mutations can be associated with different phenotypes of ARMD (not limited to the previously described cuticular drusen type). Such knowledge may ultimately lead to the development of novel therapies for this common disease. Hum Mutat 27(6), 568–574, 2006.   © 2006 Wiley-Liss, Inc.

KEY WORDS: age-related macular degeneration; ARMD; fibulin 5; FBLN5; cutis laxa; genotype–phenotype correlation; elastinogenesis

INTRODUCTION

Age-related macular degeneration (ARMD; MIM#s 603075, 153800, and 608895) is the commonest cause of irreversible visual loss in the Western world [Klaver et al., 1998; Tielsch et al., 1995], affecting approximately 25 million people worldwide (http://AMDalliance.org).

The progressive loss of central vision in ARMD occurs due to degenerative and neovascular changes within the retina at the macula. Specifically, extracellular deposits of protein and lipid develop beneath the retinal pigment epithelium (RPE) and within an elastin-containing structure known as Bruch's membrane and can be seen clinically as yellowish white spots in the retina [Ambati et al., 2003]. The RPE degenerates and choroidal neovascularization can spread through the RPE into the retina with disastrous consequences for central vision [Ambati et al., 2003].

Both environmental and genetic risk factors are known to be associated with ARMD [Christen et al., 1996; Seddon et al.,

1996]. Sequence changes in the fibulin 5, complement factor H, human leukocyte antigen (HLA), and perhaps the toll-like receptor 4 genes have all been associated with ARMD [Hageman et al., 2005; Haines et al., 2005; Edwards et al., 2005; Klein et al., 2005; Zareparsi et al., 2005; Stone et al., 2004; Goverdhan et al., 2005].

WILEY InterScience
DISCOVER SOMETHING GREAT

Previously a comprehensive analysis of fibulin 5 (FBLN5; MIM# 604580) in a cohort of 402 patients with ARMD and age-matched controls identified missense mutations in FBLN5 in 1.7% of ARMD patients recruited from the United States [Stone et al., 2004]. Due to the high prevalence of ARMD this equates to many hundreds of thousands of ARMD patients worldwide with FBLN5 mutations.

The fibulins are a family of extracellular matrix (ECM) proteins [Timpl et al., 2003] and are characterized by tandem arrays of epidermal growth factor–like (EGF-like) domains. Fibulins are widespread components of ECM and participate in diverse supramolecular structures with binding sites for several proteins including tropoelastin, fibrillin and proteoglycans. Phenotypes previously associated with mutations in fibulin genes include Malattia Leventinese and Doyne honeycomb retinal dystrophy (fibulin 3) [Stone et al., 1999], cutis laxa (fibulin 5) [Loeys et al., 2002; Markova et al., 2003], and ARMD in a single family (fibulin 6) [Schultz et al., 2003].

Fibulin 5 is a 66-kDa secreted protein of 448 amino acids [Nakamura et al., 1999]. It shares around 90% amino acid identity with other fibulin species. It is one of the shorter fibulins and has a central segment of five calcium binding EGF-like modules and a carboxy-terminal domain III of sequence identity with the other fibulins [Timpl et al., 2003]. It is widely expressed throughout the body including the RPE [Stone et al., 2004] and choroid (www.ncbi.nlm.nih.gov/UniGene). The missense FBLN5 variants identified in the ARMD patients [Stone et al., 2004] are spread along the protein with one lying very close to the arg-gly-asp (RGD) integrin binding domain (p.V60L), one affecting a calcium-binding EGF-like domain (p.I169 T), and three affecting the region thought to bind to LOXL1 (p.R351W, p.A363 T, and p.G412E) [Liu et al., 2004] .

Two groups have published a description of a fibulin 5 –/– mouse [Yanagisawa et al., 2002; Nakamura et al., 2002]. In both cases the mice exhibited a severe form of elastinopathy with loose skin, vascular abnormalities, and emphysematous lungs, demonstrating that FBLN5 is essential for elastinogenesis. Of note, Bruch's membrane, lying between the RPE and choroid, is a multilayered structure that contains a central layer of elastin, and abnormalities in this membrane play a key role in the pathogenesis of ARMD.

We chose to investigate FBLN5 variants in the European population, identified novel sequence variants, and determined their prevalence in two European cohorts of 514 patients (United Kingdom) and 288 patients (Netherlands). FBLN5 is a secreted protein which functions in the extracellular matrix [Timpl et al., 2003]. We thus evaluated whether these novel sequence variants and previously identified variants impaired secretion of mutant FBLN5 in cell culture experiments. We also determined phenotype–genotype correlations.

MATERIALS AND METHODS

At the University of Southampton a cohort of 514 ARMD patients and 188 control patients from the same clinic population were screened. All patients and control patients were over the age of 50 years and had undergone a dilated retinal examination. Mutation analysis of FBLN5 (GenBank accession number: NM_006329.2) was performed using a combination of single stranded conformation polymorphism and direct sequencing as reported previously [Lotery et al., 2000a,b, 2001]. Ethical permission for this study was obtained from the Southampton and Southwest Hants Local Research Ethics Committee (approval no. 347/02/t).

The Dutch cohort consisted of 288 unrelated Caucasian patients and 149 ethnically- and age-matched controls. Subjects were primarily recruited from the ophthalmic departments in Amsterdam and Rotterdam. All subjects underwent fundus photography. Transparencies were graded according to a modified version of the International Classification System [Bird et al., 1995]. Cases were subjects with soft distinct drusen and pigmentary irregularities, soft indistinct or reticular drusen, geographic atrophy, or neovascular macular degeneration (i.e., age-related maculopathy stages 2–4). Controls were subjects aged 65 years and older with no or only a few small hard drusen and no other macular pathology (age-related maculopathy stage 0). Control subjects were either unaffected spouses of cases, or subjects who attended the ophthalmology department for reasons other than retinal pathology. A combination of DHPLC analysis (Transgenomic, Omaha, NE; www.transgenomic.com) and direct sequencing was used for mutation analysis.

Computer-Based Predictions of Structure

The protein fold recognition program "Threader 3" [Jones et al., 1999] was used to predict the effects of missense mutations on protein folding. Threader assesses whether a test primary amino acid sequence (in this case a fibulin 5 sequence) can align with and fold like known protein structures from a library. For threading, the test sequence is divided dynamically into small segments. Threading of the test sequence upon each known structure is based on optimization of the pairwise (folding) energy sums and also the solvation energy sums. Threader generates Z-scores, which are quantitative measures of the quality of matches: Large, positive Z-scores point toward a successful prediction. Threading was not constrained by providing any predicted secondary structure for fibulin 5.

Expression of Fibulin 5 (FBLN5) in COS7 Cells

To investigate the expression of wild-type (WT) and mutant FBLN5 we generated expression constructs in pEF6-ssFLAG vector for WT FBLN5 and 13 different FBLN5 mutations. These included those mutations previously described as being associated with ARMD (p.V60L, p.R71Q, p.P87S, p.I169 T, p.R351W, p.A363 T, and p.G412E) [Stone et al., 2004], the mutations we have identified as being associated with ARMD (p.G267S, p.Q124P), one missense change we identified in a control patient without ARMD as a control (p.G202R), a mutation identified in both ARMD and control patients (p.V126 M), and two mutations previously described as causing cutis laxa (p.S227P [Loeys et al., 2002] and (p.C217R [Fischer et al., 2004]). Mutations were generated by site-directed mutagenesis using the QuikChange XL Site-Directed Mutagenesis Kit (Stratagene, La Jolla, CA; www.stratagene.com) as described [Wang et al., 2002] and the presence of each mutation was confirmed by DNA sequencing. The pEF6-ssFLAG constructs were used to transfect COS-7 cells and protein expression was induced. Nontransfected COS-7 cells do not express fibulin 5 (data not shown).

Cell Culture and Transfection

All experiments were carried out in triplicate. COS-7 cells were grown and transfected as described previously using 0.5 µg of DNA [Wang et al., 2002]. After 72 hr cells were harvested, and for Western blot analysis whole cell lysates were prepared as previously described and blotted [Wang et al., 2002]. Samples of the medium (nonconcentrated) in which the cells had grown were also blotted to detect secreted fibulin 5. The expressed tagged

fibulin 5 was detected by Anti-FLAG antibody (Sigma, Gilling-ham, Dorset, England; www.sigmaaldrich.com) and the bands were quantified using Fluor-S Max MultiImager (Biorad, Hercules, CA; www.bio-rad.com).

For each sample in all experiments we compared the secreted fibulin 5 to fibulin 5 in the cell lysate, thus allowing us to determine a ratio for each sample. We did not compare absolute measurements between samples as we were using transient transfections but, instead, we compared the ratios of cell lysate and medium fibulin 5 for each mutant fibulin 5 construct with the ratio for the WT fibulin5 constructs.

RESULTS

Two novel heterozygous missense mutations were identified solely in three United Kingdom patients (p.Q124P in one patient and p.G267S in two apparently unrelated patients). No sequence variations were found in patients alone in the Netherlands cohort (Table 1). Two missense changes were identified in controls (p.V126 M found in 5 controls and 1 ARMD patient and p.G202R found in a control individual), suggesting these changes are polymorphic sequence variants.

We used the protein fold recognition program Threader 3 to predict the effects on protein folding of these missense sequence changes together with those previously published in ARMD patients [Stone et al., 2004], the missense changes identified in control individuals (p.V126 M, p.G202R) and two mutations previously described in cutis laxa (p.S227P, p.C217R) [Loeys et al., 2002; Fischer et al., 2004]. The structure 1l0qa0 (391 residues)

was the best match both 1) when the WT fibulin 5 sequence (448 residues) was threaded using default parameter values against each of the 6251 structures in the reference library (Z = 6.8, statistically very significant); and 2) when the top 15 matches from (1) were subjected to randomization tests (using the option r50), which identify true-positive matches and eliminate false-positives. A prediction of the effects on folding of each mutation was obtained indirectly by comparing the results from threading the mutant against 1l0qa0 with those from threading the WT against the same structure. Table 2 presents the threading energies, the Z-scores (which indicate the quality of matches), and the alignments for WT and each mutation. Of note, both the cutis laxa mutation p.C217R and the ARMD-associated change p.Q124P reduce the magnitude of the pairwise (folding) energy sum by > 2.5%, and reduce the corresponding Z-score. For p.Q124P, compensation for the change in folding energy (Table 2; column 2) by an opposing change in solvation energy (column 4) leads to virtually no change in the total energy (column 6) and its Z-score (column 7). For p.C217R, the changes in pairwise and solvation energies are synergistic, leading to a reduction of the magnitude of total energy by > 2.5%. The two mutations p.G267S and p.R351W improve the stability on folding by > 2.5%, and with reduced percentage alignments.

Changes in protein folding might interfere with secretion of the protein and to test this we expressed each of the sequence variants and WT fibulin 5 in COS7 cells together with those previously published in ARMD patients [Stone et al., 2004], the missense changes identified in control individuals (p.V126 M, p.G202R) and two mutations previously described in cutis laxa (p.S227P,

TABLE 1. Sequence Variations in the FBLN5 Gene*

	Nucleotide change		Effect or sequence change		Degree of conservation[a]
Amino acid changing variants					
United Kingdom data			ARMD (n = 514)	Controls (n = 188)	
Exon 4	c.371A > C	p.Gln124Pro	1	0	8/8, chicken
Exon 6	c.604G > A	p.Gly202Arg	0	1	11/11, chicken
Exon 8	c.799G > A	p.Gly267Ser	2	0	10/10, chicken
Netherlands data			ARMD (n = 291)	Controls (n = 91)	
Exon 4	c.376G > A	p.Val126Met	1	5	7/8, bovine
Synonymous coding variants					
United Kingdom data			ARMD affected (n = 514)	Controls (n = 188)	
Exon 5	c.484C > T	p.Leu162Leu	1	0	
Exon 9	c.945T > C	p.Ile315Ile	206	76	
Exon 10	c.1122C > T	p.Tyr374Tyr	19	10	
Exon 10	c.1134T > C	p.Tyr378Tyr	2	0	
Netherlands data			ARMD (n = 291)	Controls (n = 91)	
Exon 7	c.735C > T	p.Cys245Cys	2	0	
Exon 9	c.945T > C	p.Ile315Ile	99	37	
Exon 10	c.1122C > T	p.Tyr374Tyr	18	7	
Intronic variants					
United Kingdom data		ARMD (n = 514)	Controls (n = 188)		
Intron 3	c.125-53G > A	1	0		
Intron 3	c.125-45G > C	5	1		
Netherlands data		ARMD (n = 291)	Controls (n = 91)		
5'UTR	c.1-33C > A	1	0		
Intron 1	c.18-28A > G	21	8		
3'UTR	c.1347 + 97G > A	0	1		
3'UTR	c.1347 + 121C > T	1	0		
3'UTR	c.1347 + 352G > C	15	28		
3'UTR	c.1347 + 423T > C	7	6		
3'UTR	c.1347 + 514A > G	18	38		

*Degree of conservation values are the number of nonhuman species that share this residue with humans. The species with the greatest phylogenic distance from humans with a sequence that is homologous to that of humans is also given. cDNA numbering is taken from Ref Seq # NM_006329.2 where +1 corresponds to the A of the ATG initiation codon.
[a]Number of conserved variations/total number of variations.

TABLE 2. "Threading" of the Fibulin 5 Mutants Against the Structure 1l0qa0*

1	2	3	4	5	6	7	8	9	10	11	12	13
WT	−1026	6.80	−7.81	2.41	−1214	6.14	157.3	359	92.3	80.4		→
V60L[a]	−1021	6.77	−7.82	2.42	−1210	6.14	155.9	359	92.3	80.4	IE	→
R71Q[a]	−1026	6.80	−7.77	2.41	−1213	6.13	156.9	359	92.3	80.4	IC	→
P87S[a]	−1031	6.84	−7.81	2.44	−1222	6.21	158.5	359	92.3	80.4	IE	→
Q124P[a]	−970	6.39	−9.75	2.78	−1207	6.10	174.8	359	92.3	80.4	IE	↓↓
V126M[a]	−1010	6.74	−7.77	2.41	−1197	6.12	160.0	359	92.3	80.4	IE	→
I169T[a]	−1018	6.77	−8.46	2.54	−1224	6.16	157.2	359	92.3	80.4	IE	↓
G202R[b]	−1026	6.84	−8.20	2.51	−1225	6.27	158.6	359	92.3	80.4	IC	→
C217R[c]	−986	6.62	−6.76	2.23	−1148	5.88	155.2	359	92.3	80.4	IE	↓↓
S227P[c]	−1026	6.87	−7.77	2.40	−1211	6.13	159.0	359	92.3	80.4	IC	↓↓
G267S[a]	−1036	6.93	−10.03	2.85	−1279	6.56	190.4	354	90.8	79.0	IC	↓
R351W[a]	−1026	6.76	−9.55	2.75	−1258	6.34	175.8	357	91.8	79.9	IC	→
A363T[a]	−1026	6.79	−8.06	2.44	−1221	6.15	158.4	359	92.3	80.4	IC	→
G412E[a]	−1026	6.83	−7.81	2.42	−1215	6.18	157.3	359	92.3	80.4	O	↓

*Threading of the test fibulin 5 sequences (column 1) upon 1l0qa0 is based on optimization of the pairwise energy sums and the solvation energy sums. The raw pairwise energy sum (kcal mol^{-1}, column 2) is adjacent to its corresponding Z-score (column 3). The raw solvation energy sum (kcal mol^{-1}, column 4) is adjacent to its Z-score (column 5). The sum of pairwise and solvation energies (column 6), weighted as described in the Threader documentation, is given with its Z-score (column 7). The high sequence-similarity scores (column 8) might indicate common ancestry between 1l0qa0 and fibulin 5. In addition, the number of residues (column 9) and the exceptionally high percentages of 1l0qa0 (column 10) and fibulin 5 (column 11) that were aligned are listed. Column 12 lists whether a mutation is inside (I) or outside (O) the alignment, and the 1l0qa0 secondary structure (E, extended; C, coil) at that point. Column 13 summarizes the secretion data (Fig. 1). Deviations > 2.5% from figures obtained for wild-type fibulin 5 are shown in bold. Changes in the alignments are shown in italics. Z-scores are quantitative measures of the quality of matches. Large and positive Z-scores point toward a successful prediction: Z > 4.0, very significant, indicating probably a correct prediction; 4.0 > Z > 3.5, significant with a good chance of being correct; 3.5 > Z > 2.7, borderline; 2.7 > Z > 2.0, poor; 2.0 > Z, very poor.
[a]Mutations associated with ARMD.
[b]Missense change identified in a control patient without ARMD.
[c]Mutations associated with cutis laxa.

p.C217R) [Loeys et al., 2002; Fischer et al., 2004]. Western blot analysis following harvesting of the transfected cells indicated WT fibulin 5 was present both in whole cell lysates and in the medium from the cell culture (Fig. 1A), confirming that fibulin 5 is secreted by these cells. The ratio of fibulin 5 detected in the medium compared to that in the whole cell lysate for 6 of the 11 disease-associated mutations was significantly reduced (P < 0.001) (Fig. 1B) indicating a reduction in secretion for these mutant forms of fibulin 5 but no change in secretion was noted for the two sequence variants identified in controls. Four of these mutations are associated with ARMD (p.G412E, p.G267S, p.I169 T, and p.Q124P) and two have been found to cause cutis laxa (p.S227P, p.C217R) (Fig. 1B).

Genotype–Phenotype Correlation

Two of the three Southampton patients had a clinical phenotype of cuticular drusen. Patient 1 (p.Q124P) had small round uniform drusen but no choroidal neovascularization and no evidence of pigment epithelial detachments. Patient 2 (p.G267S) had pure choroidal neovascularization in one eye but no drusen. Patient 3 (p.G267S) had cuticular drusen and central localized pigment epithelial detachments. (Fig. 2).

DISCUSSION

This study identified novel heterozygous fibulin 5 mutations in 3 out of 514 UK patients with ARMD, a prevalence of 0.6%. In the Netherlands cohort, however, we found no fibulin 5 sequence variants specific to patients. Previously, missense FBLN5 mutations were identified in 7 out of 402 U.S. patients with ARMD (1.7%) [Stone et al., 2004] and these mutations were proposed to result in an increased susceptibility to ARMD. The work we describe here is the first similar study in a different population of ARMD patients. The results from the UK cohort support the hypothesis that a number of rare FBLN5 variants are unique for ARMD patients, which suggests these mutations may affect fibulin

5 function. The results from the Netherlands cohort might reflect the lower number of patients studied or genetic founder effects specific for the Dutch population. It is well recognized that the first report [Stone et al., 2004] describing an association between a gene and a disease often overestimates the fraction of disease caused by mutation in the gene in question [Ioannidis et al., 2001] and these results would suggest this may be a factor here. Again this emphasizes the need for subsequent studies such as ours, both to assess the effect in further populations and also to further investigate the biological consequences of the genetic mutations.

The statistical association of sequence variants with a multifactorial condition such as ARMD is only the first step in determining any causative relationship. Fibulin 5 is a secreted extracellular matrix protein that has a role in elastinogenesis through interactions with integrins [Nakamura et al., 2002], tropoelastin [Tsuruga et al., 2004], and LOXL1 [Liu et al., 2004]. Missense mutations affecting protein folding might interfere with fibulin 5 moving through the secretory pathway or with subsequent protein interactions. Interference with protein trafficking and secretion is an increasingly recognized mechanism by which missense mutations cause genetic disease [Aridor and Hannan, 2000]. It is thought to occur when the missense mutation leads to abnormal protein folding, thus inducing the "unfolded protein response" in the endoplasmic reticulum, leading to intracellular degradation of the mutant protein; and it can occur with missense changes at different points in a protein [Aridor and Hannan, 2000].

We hypothesized that the missense mutations in fibulin 5 may lead to susceptibility to ARMD due to reduced fibulin 5 secretion; as an initial approach to investigating this we modeled the effects of mutations on protein folding using Threader 3. These results suggested some sequence variants might affect folding and thus potentially secretion of mutant protein. We therefore expressed WT and mutant forms of fibulin 5 and compared secretion. Six sequence changes did indeed interfere with secretion and four of these were predicted to interfere with folding. In contrast, other

A.

B.

Comparison of mutant Fibulin 5 secretion

* P < 0.001
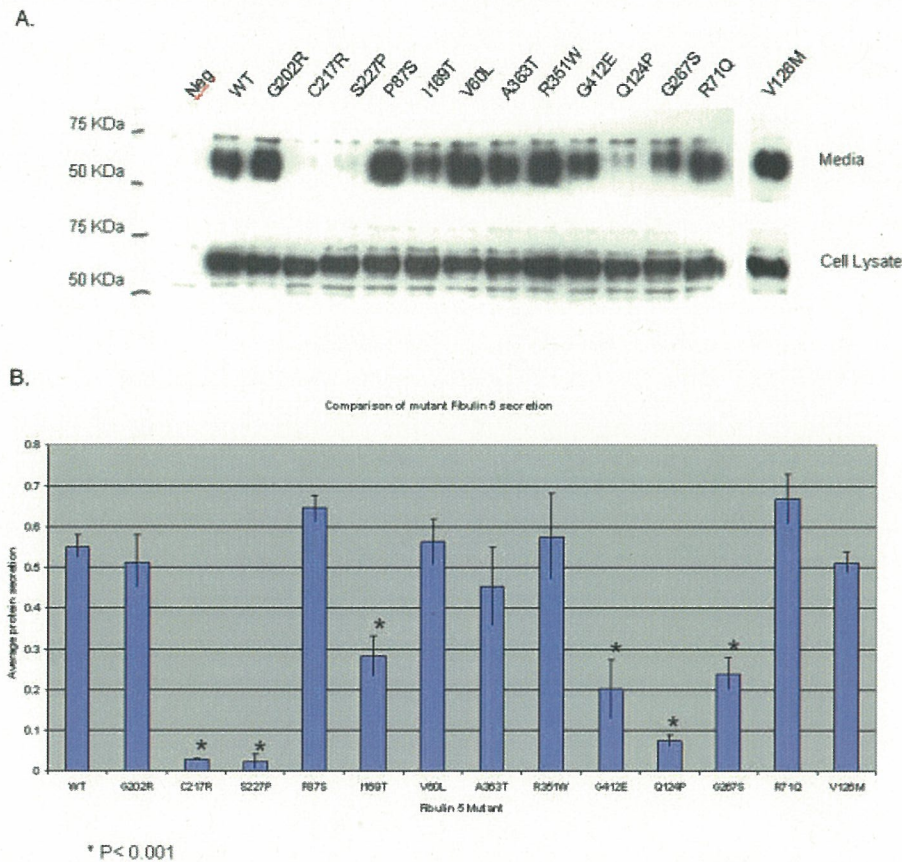
FIGURE 1. **A:** Secretion of WT and mutant forms of fibulin 5. WT and mutant fibulin 5 were expressed in transfected COS-7 cells. At 72 hr after transfection, cell lysate and medium samples were prepared and separated by 10% SDS–polyacrylamide gels followed by immunoblotting. These included WT, two mutations previously associated with cutis laxa (p.C217R and p.S227P), mutations previously associated with ARMD (p.R71Q, p.P87S, p.I169 T, p.V60L, p.A363 T, p.R351W, and p.G412E), novel mutations we identified in ARMD patients (p.Q124P, p.G267S), and two control missense mutations (p.V126 M, p.G202R). **B:** Quantification of secreted fibulin 5. For WT and each mutation the ratio of secreted fibulin 5 to fibulin 5 in the cell lysate was calculated. These were compared between WT and each mutations and results analyzed using Student's t-test. *P < 0.001.

sequence changes were also predicted to change protein folding but did not change secretion. This may indicate protein folding changes that did not activate the unfolded protein response or, alternatively, reflect the limitations of computer modeling.

Mutations leading to autosomal recessive cutis laxa caused a dramatic reduction in secretion of fibulin 5 when compared with WT (P < 0.001) and a similar reduction in secretion was observed for four of the nine mutations associated with ARMD (p.G412E, p.G267S, p.I169 T, and p.Q124P). In vitro expression studies such as these are often the first indication of missense mutations reducing protein secretion and thus causing a phenotype. Fibulin 5 is moderately expressed by the human RPE and not by the photoreceptors [Simone van Soest et al., personal communication] and therefore fibulin 5 through its role in elastinogenesis may contribute to the maintenance of the integrity of Bruch's membrane in the eye. Correspondingly, a reduction in secretion might interfere with this.

Several members of the fibulin gene family have been associated with macular degeneration. In previous studies by Stone et al. [2004] and other groups [Schultz et al., 2003], variations in other fibulins (fibulin-1, 2, 4, and 6) were also reported specifically associated with ARMD patients. In addition, a mutation in fibulin-3 causes a more severe form of macular degeneration (earlier onset), Malattia Leventinese or Doyne honeycomb retinal dystrophy with high similarities to ARMD [Stone et al., 1999].

Although no fibulin-3 mutation has been found in ARMD, the fibulin 3 protein accumulates in Bruch's membrane in ARMD [Marmorstein et al., 2002]. Secretion of mutant fibulin-3 is also significantly reduced [Marmorstein et al., 2002]. The FBLN5 gene is not highly polymorphic and the identification of new mutations in different ARMD cohorts but not in control populations (this study and the previous one by Stone et al., 2004) suggests that the missense sequence changes have a functional effect on fibulin 5 function and that there is a causal relationship between FBLN5 and the pathogenesis of ARMD rather then this being a chance association. This study further demonstrates that FBLN5 mutations can be associated with different phenotypes of ARMD (not limited to cuticular druse type).

Our results suggest that some missense mutations associated with ARMD lead to decreased fibulin 5 secretion. Since fibulin 5 is essential for elastinogenesis, our hypothesis is that this reduced secretion in turn results in a corresponding reduction in elastinogenesis. However, this is as yet unconfirmed for the ARMD related mutations and requires further investigation.

It is particularly noteworthy that one of the ARMD associated mutations (p.Q124P) leads to a similar reduction in secretion to the two mutations known to cause cutis laxa in which elastinogenesis is disrupted [Loeys et al., 2002; Fischer et al., 2004]. This raises the possibility that patients with this form of cutis laxa may have early onset ARMD, and their parents
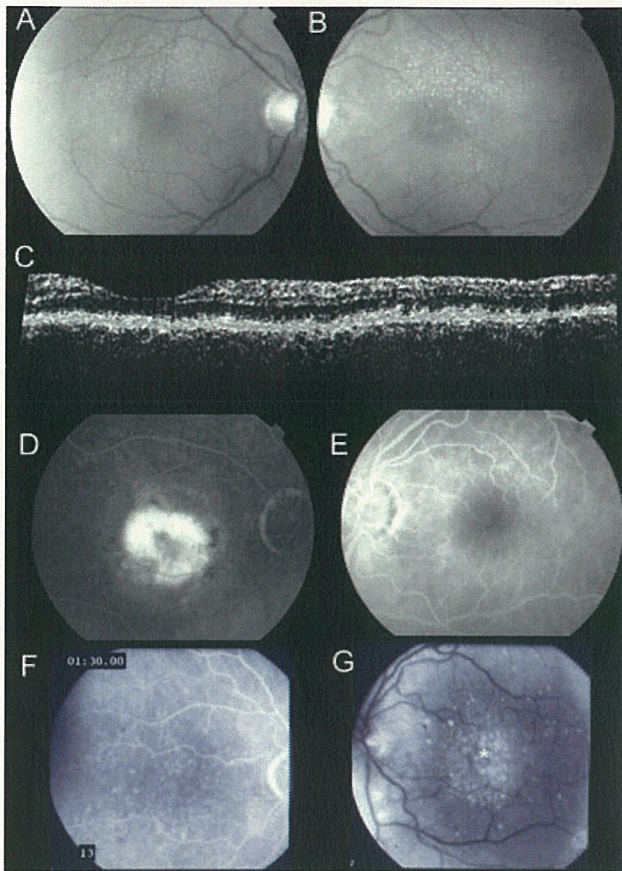
FIGURE 2. **A,B:** Retinal photographs of Patient 1 (p.Q124P). Small round (cuticular) drusen are symmetrically present. **C:** Optical coherence tomogram of Patient 1 demonstrates nodular thickening of the retinal pigment epithelium (*). **D,E:** Fluorescein angiograms of Patient 2 (p.G267S) demonstrate choroidal neovascularization in one eye only. **F,G:** Fluorescein angiogram photographs of Patient 3 (p.G267S) demonstrate cuticular drusen with central areas of focal retinal pigment epithelial detachment (*).

2004]. We have observed this same phenotype in two of our three patients with novel FBLN 5 mutations. However, interestingly, two patients with the same p.G267S sequence change demonstrated markedly different phenotypes. Such variation in retinal phenotype has been well described before in monogenetic retinal diseases [Weleber et al., 1993]. FBLN5 ARMD can therefore also be a cause of choroidal neovascularization in the absence of drusen.

This study identifies a mechanism by which FBLN5 mutations can lead to ARMD. Such knowledge should ultimately lead to the development of novel therapies for this devastating disease. It also expands the retinal phenotypes associated with FBLN5 mutations and identifies the prevalence of ARMD in two European cohorts. Such information will be valuable for future gene directed therapies.

ACKNOWLEDGMENTS

REFERENCES

Ambati J, Ambati BK, Yoo SH, Ianchulev S, Adamis AP. 2003. Age-related macular degeneration: etiology, pathogenesis, and therapeutic strategies. Surv Ophthalmol 48:257–293.

AREDS Research Group. 2001. A randomized, placebo-controlled, clinical trial of high-dose supplementation with vitamins C and E, beta carotene, and zinc for age- related macular degeneration and vision loss: AREDS report no. 8. Arch Ophthalmol 119:1417–1436.

Aridor M, Hannan LA. 2000. Traffic jam: a compendium of human diseases that affect intracellular transport processes. Traffic 1:836–851.

Bird AC, Bressler NM, Bressler SB, Chisholm IH, Coscas G, Davis MD, de Jong PT, Klaver CC, Klein BE, Klein R, Mitchell P, Sarks JP, Sarks SH, Soubrane G, Taylor H, Vingerling JR. 1995. An international classification and grading system for age- related maculopathy and age-related macular degeneration. The International ARM Epidemiological Study Group. Surv Ophthalmol 39:367–374.

Christen WG, Glynn RJ, Manson JE, Ajani UA, Buring JE. 1996. A prospective study of cigarette smoking and risk of age-related macular degeneration in men. JAMA 276:1147–1151.

Edwards AO, Ritter R, III, Abel KJ, Manning A, Panhuysen C, Farrer LA. 2005. Complement factor H polymorphism and age-related macular degeneration. Science 308:421–424.

Fischer J, Jobard F, Oudot T, Geneviève D, Mégarbané A, Pauchard J, Saker S, Godeau G, Damour O, Peyrol S, Blanchet-Bardon C, de Prost Y, Hadj-Rabia S, Devillers M, Sommer P. 2004. Identification of novel mutations in elastin and fibulin 5 in three patients affected with cutis laxa. Third European Symposium Elastin. 2004. 30th June–3rd July 2004, Manchester, UK.

Goverdhan SV, Howell MW, Mullins RF, Osmond C, Hodgkins PR, Self J, Avery K, Lotery AJ. 2005. Association of HLA class I and class II polymorphisms with age-related macular degeneration. Invest Ophthalmol Vis Sci 46:1726–1734.

(heterozygous for these mutations) may themselves be at a higher risk of ARMD than the general population. Furthermore, these ARMD FBLN5 sequence variants may lead to cutis laxa if inherited as homozygous mutations and the ARMD patients in whom we have identified a sequence variant in fibulin 5 may be "carriers" for cutis laxa. We have found reduced secretion of FBLN5 for both cutis laxa mutations and for some ARMD mutations. This suggests there may be a relationship between dose of fibulin 5 and disease severity. Homozygous mutations may interfere with elastinogenesis and result in the early onset cutis laxa phenotype, whereas heterozygous mutations may result in a later onset phenotype of ARMD. Environmental stresses such as smoking may also influence the development of the ARMD late onset phenotype. Further studies investigating the effects of these variants and gene–environment interactions will be important. Not only to clarify how they may affect fibulin 5 function, but also to determine whether we should give lifestyle advice for the parents of patients with cutis laxa and consider additional ophthalmologic supervision and possible early treatment for these individuals with vitamin supplements [AREDS Research Group, 2001].

Previously, FBLN 5 associated ARMD has been associated with a specific retinal phenotype of cuticular drusen [Stone et al.,

Hageman GS, Anderson DH, Johnson LV, Hancox LS, Taiber AJ, Hardisty LI, Hageman JL, Stockman HA, Borchardt JD, Gehrs KM, Smith RJH, Silvestri G, Russell SR, Klaver CCW, Barbazetto I, Chang S, Yannuzzi LA, Barile GR, Merriam JC, Smith RT, Olsh AK, Bergeron J, Zernant J, Merriam JE, Gold B, Dean M, Allikmets R. 2005. From the cover: a common haplotype in the complement regulatory gene factor H (HF1/CFH) predisposes individuals to age-related macular degeneration. Proc Natl Acad Sci USA 102:7227–7232.

Haines JL, Hauser MA, Schmidt S, Scott WK, Olson LM, Gallins P, Spencer KL, Kwan SY, Noureddine M, Gilbert JR, Schnetz-Boutaud N, Agarwal A, Postel EA, Pericak-Vance MA. 2005. Complement factor H variant increases the risk of age-related macular degeneration. Science 308:419–421.

Ioannidis JP, Ntzani EE, Trikalinos TA, Contopoulos-Ioannidis DG. 2001. Replication validity of genetic association studies. Nat Genet 29:306–309.

Jones DT, Tress M, Bryson K, Hadley C. 1999. Successful recognition of protein folds using threading methods biased by sequence similarity and predicted secondary structure. Proteins Suppl 3:104–111.

Klaver CC, Wolfs RC, Vingerling JR, Hofman A, de Jong PT. 1998. Age-specific prevalence and causes of blindness and visual impairment in an older population: the Rotterdam Study. Arch Ophthalmol 116:653–658.

Klein RJ, Zeiss C, Chew EY, Tsai JY, Sackler RS, Haynes C, Henning AK, Sangiovanni JP, Mane SM, Mayne ST, Bracken MB, Ferris FL, Ott J, Barnstable C, Hoh J. 2005. Complement factor H polymorphism in age-related macular degeneration. Science 308:385–389.

Liu X, Zhao Y, Gao J, Pawlyk B, Starcher B, Spencer JA, Yanagisawa H, Zuo J, Li T. 2004. Elastic fiber homeostasis requires lysyl oxidase-like 1 protein. Nat Genet 36:178–182.

Loeys B, Van Maldergem L, Mortier G, Coucke P, Gerniers S, Naeyaert JM, De Paepe A. 2002. Homozygosity for a missense mutation in fibulin-5 (FBLN5) results in a severe form of cutis laxa. Hum Mol Genet 11:2113–2118.

Lotery AJ, Munier FL, Fishman GA, Weleber RG, Jacobson SG, Affatigato LM, Nichols BE, Schorderet DF, Sheffield VC, Stone EM. 2000a. Allelic variation in the VMD2 gene in best disease and age-related macular degeneration. Invest Ophthalmol Vis Sci 41:1291–1296.

Lotery AJ, Namperumalsamy P, Jacobson SG, Weleber RG, Fishman GA, Musarella MA, Hoyt CS, Heon E, Levin A, Jan J, Lam B, Carr RE, Franklin A, Radha S, Andorf JL, Sheffield VC, Stone EM. 2000b. Mutation analysis of 3 genes in patients with Leber congenital amaurosis. Arch Ophthalmol 118:538–543.

Lotery AJ, Malik A, Shami SA, Sindhi M, Chohan B, Maqbool C, Moore PA, Denton MJ, Stone EM. 2001. CRB1 mutations may result in retinitis pigmentosa without para- arteriolar RPE preservation. Ophthalmic Genet 22:163–169.

Markova D, Zou Y, Ringpfeil F, Sasaki T, Kostka G, Timpl R, Uitto J, Chu ML. 2003. Genetic heterogeneity of cutis laxa: a heterozygous tandem duplication within the fibulin-5 (FBLN5) gene. Am J Hum Genet 72:998–1004.

Marmorstein LY, Munier FL, Arsenijevic Y, Schorderet DF, McLaughlin PJ, Chung D, Traboulsi E, Marmorstein AD. 2002. Aberrant accumulation of EFEMP1 underlies drusen

formation in Malattia Leventinese and age-related macular degeneration. Proc Natl Acad Sci USA 99:13067–13072.

Nakamura T, Ruiz-Lozano P, Lindner V, Yabe D, Taniwaki M, Furukawa Y, Kobuke K, Tashiro K, Lu Z, Andon NL, Schaub R, Matsumori A, Sasayama S, Chien KR, Honjo T. 1999. DANCE, a novel secreted RGD protein expressed in developing, atherosclerotic, and balloon-injured arteries. J Biol Chem 274:22476–22483.

Nakamura T, Lozano PR, Ikeda Y, Iwanaga Y, Hinek A, Minamisawa S, Cheng CF, Kobuke K, Dalton N, Takada Y, Tashiro K, Ross J, Jr, Honjo T, Chien KR. 2002. Fibulin-5/DANCE is essential for elastogenesis in vivo. Nature 415:171–175.

Schultz DW, Klein ML, Humpert AJ, Luzier CW, Persun V, Schain M, Mahan A, Runckel C, Cassera M, Vittal V, Doyle TM, Martin TM, Weleber RG, Francis PJ, Acott TS. 2003. Analysis of the ARMD1 locus: evidence that a mutation in HEMI-CENTIN-1 is associated with age-related macular degeneration in a large family. Human Molecular Genetics 12:3315–3323.

Seddon JM, Willett WC, Speizer FE, Hankinson SE. 1996. A prospective study of cigarette smoking and age-related macular degeneration in women. JAMA 276:1141–1146.

Stone EM, Lotery AJ, Munier FL, Heon E, Piguet B, Guymer RH, Vandenburgh K, Cousin P, Nishimura D, Swiderski RE, Silvestri G, Mackey DA, Hageman GS, Bird AC, Sheffield VC, Schorderet DF. 1999. A single EFEMP1 mutation associated with both Malattia Leventinese and Doyne honeycomb retinal dystrophy. Nat Genet 22:199–202.

Stone EM, Braun TA, Russell SR, Kuehn MH, Lotery AJ, Moore PA, Eastman CG, Casavant TL, Sheffield VC. 2004. Missense variations in the fibulin 5 gene and age-related macular degeneration. N Engl J Med 351:346–353.

Tielsch JM, Javitt JC, Coleman A, Katz J, Sommer A. 1995. The prevalence of blindness and visual impairment among nursing home residents in Baltimore. N Engl J Med 332:1205–1209.

Timpl R, Sasaki T, Kostka G, Chu ML. 2003. Fibulins: a versatile family of extracellular matrix proteins. Nat Rev Mol Cell Biol 4:479–489.

Tsuruga E, Yajima T, Irie K. 2004. Induction of fibulin-5 gene is regulated by tropoelastin gene, and correlated with tropoelastin accumulation in vitro. Int J Biochem Cell Biol 36:395–400.

Wang T, Waters CT, Rothman AM, Jakins TJ, Romisch K, Trump D. 2002. Intracellular retention of mutant retinoschisin is the pathological mechanism underlying X-linked retinoschisis. Hum Mol Genet 11:3097–3105.

Weleber R, Carr R, Murphey W, Sheffield V, Stone E. 1993. Phenotypic variation including retinitis pigmentosa, pattern dystrophy, and fundus flavimaculatus in a single family with a deletion of the codon 153 or 154 of the peripherin/RDS gene. Arch Ophthalmol 111:1531–1542.

Yanagisawa H, Davis EC, Starcher BC, Ouchi T, Yanagisawa M, Richardson JA, Olson EN. 2002. Fibulin-5 is an elastin-binding protein essential for elastic fibre development in vivo. Nature 415:168–171.

Zareparsi S, Buraczynska M, Branham KE, Shah S, Eng D, Li M, Pawar H, Yashar BM, Moroi SE, Lichter PR, Petty HR, Richards JE, Abecasis GR, Elner VM, Swaroop A. 2005. Toll-like receptor 4 variant D299G is associated with susceptibility to age-related macular degeneration Hum Mol Genet 14:1449–1455.

Targeted Disruption of Fibulin-4 Abolishes Elastogenesis and Causes Perinatal Lethality in Mice

Precious J. McLaughlin,[1]† Qiuyun Chen,[1]† Masahito Horiguchi,[2] Barry C. Starcher,[3] J. Brett Stanton,[1]
Thomas J. Broekelmann,[4] Alan D. Marmorstein,[1,5] Brian McKay,[1,6] Robert Mecham,[4]
Tomoyuki Nakamura,[2] and Lihua Y. Marmorstein[1,6,7]*

Department of Ophthalmology and Vision Science,[1] Optical Sciences Center,[5] Department of Cell Biology and Anatomy,[6]
and Department of Physiology,[7] University of Arizona, Tucson, Arizona; Horizontal Medical Research Organization,
Kyoto University School of Medicine, Kyoto, Japan[2]; Department of Biochemistry, University of
Texas Health Center at Tyler, Texas[3]; and Department of Cell Biology and Physiology,
Washington University School of Medicine, St. Louis, Missouri[4]

Elastic fibers provide tissues with elasticity which is critical to the function of arteries, lungs, skin, and other dynamic organs. Loss of elasticity is a major contributing factor in aging and diseases. However, the mechanism of elastic fiber development and assembly is poorly understood. Here, we show that lack of fibulin-4, an extracellular matrix molecule, abolishes elastogenesis. fibulin-4$^{-/-}$ mice generated by gene targeting exhibited severe lung and vascular defects including emphysema, artery tortuosity, irregularity, aneurysm, rupture, and resulting hemorrhages. All the homozygous mice died perinatally. The earliest abnormality noted was a uniformly narrowing of the descending aorta in fibulin-4$^{-/-}$ embryos at embryonic day 12.5 (E12.5). Aorta tortuosity and irregularity became noticeable at E15.5. Histological analysis demonstrated that fibulin-4$^{-/-}$ mice do not develop intact elastic fibers but contain irregular elastin aggregates. Electron microscopy revealed that the elastin aggregates are highly unusual in that they contain evenly distributed rod-like filaments, in contrast to the amorphous appearance of normal elastic fibers. Desmosine analysis indicated that elastin cross-links in fibulin-4$^{-/-}$ tissues were largely diminished. However, expression of tropoelastin or lysyl oxidase mRNA was unaffected in fibulin-4$^{-/-}$ mice. In addition, fibulin-4 strongly interacts with tropoelastin and colocalizes with elastic fibers in culture. These results demonstrate that fibulin-4 plays an irreplaceable role in elastogenesis.

Elastic fibers with morphologically distinct architectures are present in the extracellular matrix (ECM) to accommodate elastic requirements and mechanical stresses imposed on different tissues. They are particularly abundant in elastic tissues such as large blood vessels, lung, and skin. Loss of elasticity is a major contributing factor in aging and a myriad of pathological conditions including emphysema, artery diseases, and cutis laxa (39, 41, 44). Elastic fibers undergo irreversible structural and compositional changes with age and in some pathological conditions (41). Regardless of morphology, all elastic fibers consist of cross-linked elastin, fibrillin-rich microfibrils, and several associated molecules (23, 37, 38, 46). Elastin endows the fiber with the characteristic property of elastic recoil. It is chemically inert, extremely hydrophobic, and insoluble under most conditions. Monomeric elastin, called tropoelastin, is secreted from the cell as a soluble protein. Isolated and purified tropoelastin has been shown to exhibit a great tendency to aggregate (coacervation) in physiological solution and at temperatures in the physiological range, giving rise to supramolecular structures very similar to those found in natural elastic fibers (4, 5, 11). This self-aggregation property of tropoelastin is thought to contribute to elastic fiber assembly in vivo. However, self-aggregation alone is insufficient to explain the effi-

ciency of the assembly process and the variable form of elastic fibers in different tissues.

The formation of elastic fibers has been proposed to require the deposition of tropoelastin on a preexisting scaffold, cross-linking of tropoelastin monomers by lysyl oxidase (LOX) family enzymes, and organization of the resulting insoluble elastin matrix into mature fibers (37). Fibrillin-rich microfibrils are thought to provide the scaffold for the deposition of elastin. Unexpectedly, normal elastic fiber assembly was found to occur in fibrillin-1 or fibrillin-2 mutant mice (2, 9, 42, 43). Therefore, the molecular mechanism of elastic fiber assembly remains elusive.

A significant insight into elastogenesis comes from two recent studies of fibulin-5$^{-/-}$ mice. These mice exhibit disrupted and disorganized elastic fibers throughout the body, indicating that fibulin-5 (also known as DANCE or EVEC) plays an important role in elastic fiber formation (40, 56). fibulin-5$^{-/-}$ mice grow to adulthood without lethality but have loose skin, vascular abnormalities, and emphysematous lungs. Fibulin-5 has an RGD motif and interacts with cell surface integrins and elastin. Thus, it has been proposed to promote elastic fiber formation by linking elastic fibers to cells (40, 56).

Fibulin-5 belongs to the fibulin family of six known ECM proteins that share tandem arrays of calcium-binding epidermal growth factor domains and a characteristic carboxyl-terminal fibulin domain (1, 10, 15, 52). Although little is known about the functions of fibulins, mutations of individual members have been associated with several diseases. A single mutation of an arginine to trypotophan in fibulin-3 (also known as

---

* Corresponding author. Mailing address: Department of Ophthalmology and Vision Science, University of Arizona, 655 N. Alvernon Way, Suite 108, Tucson, AZ 85711. Phone: (520) 626-0447. Fax: (520) 626-0457. E-mail: Lmarmorstein@eyes.arizona.edu.
† P.J.M. and Q.C. contributed equally to this work.

EFEMP1, S1-5, or FBNL) causes an inherited macular degenerative disease termed malattia leventinese or Doyne honeycomb retinal dystrophy (51). Missense variations in other fibulins have been detected in patients with age-related macular degeneration (47, 50), the most common cause of incurable blindness (6). Mutations in fibulin-5 have also been found in some cutis laxa patients (29, 32). So far, fibulin-5 is the only fibulin reported to be necessary for elastogenesis, whereas fibulin-1-null mice are reported to die perinatally as a result of hemorrhages, due to defects associated with capillary endothelial cells (25). Knockout mice for other fibulins have not been reported. Among the fibulins, fibulin-3, fibulin-4 (also known as EFEMP2, MBP1, H411, or UPH1), and fibulin-5 share highest homology with each other. These three fibulins are the smallest members of the family, share >50% amino acid identity, and are nearly identical in their structural organization (1, 10, 15, 52). Despite this homology, fibulin-5 deficiency is not compensated for by fibulin-3 or -4, suggesting that fibulin-3, -4, and -5 are not functionally redundant.

The function of fibulin-4 is poorly understood. Several studies have consistently found that fibulin-4 promotes cell growth, exhibits oncogenic properties, and is upregulated in tumor tissues (14, 16, 19). *fibulin-4* mRNA has been shown to be widely expressed in various tissues throughout the body (14, 16, 18). High protein levels are present in blood vessel walls (18). During development, *fibulin-4* mRNA is expressed in mouse embryos as early as embryonic day 7 (E7) (14). In this study, we investigated the biological role of fibulin-4 through targeted gene inactivation in mice. Remarkably, mice lacking fibulin-4 do not form elastic fibers, with resulting severe vascular and lung defects; they die perinatally. These results demonstrate that fibulin-4 plays an irreplaceable role in elastic fiber formation.

MATERIALS AND METHODS

fibulin-4$^{-/-}$ **mouse generation, Southern blot analysis, and RT-PCR.** The targeting vector was constructed using 2.5-kb (5′) and 3-kb (3′) mouse *fibulin-4* genomic DNA fragments as homology arms. The two arms flanked a promoterless *lacZ* and a neomycin-resistant gene cassette (*lacZ-neo*). Homologous recombination in mouse embryonic stem cells resulted in the insertion of the *lacZ-neo* cassette into exon 4 of the mouse *fibulin-4* locus. Germ line-transmitting chimeric mice generated from the targeted embryonic stem cells were bred with C57BL/6 mice to produce F_1 *fibulin-4$^{+/-}$* mice (Deltagen). Intercrossing of heterozygous F_1 mice generated F_2 *fibulin-4$^{-/-}$* mice. Southern blot analysis was performed for identification of homologous recombinants. Genomic DNA was extracted using a DNA purification kit (Gentra) from mouse tail biopsy samples, digested with KpnI, separated on a 0.5% SeaKem Gold agarose (Cambrex) gel, and transferred to a Hybond-N$^+$ nylon membrane (Amersham) by capillary blotting. The membrane was hybridized with a 5′ or 3′ external probe that is outside of the homologous arm regions. The probes were labeled with ^{32}P through random priming using the Megaprime DNA Labeling system (Amersham). The labeled probes were purified using ProbeQuant G-50 Micro Columns (Amersham). Hybridization was performed using the MiracleHyb hybridization solution (Stratagene) according to the manufacturer's instructions. Reverse transcription-PCR (RT-PCR) was performed as described previously (33) to confirm the absence of *fibulin-4* expression in homozygous mice. Total RNA was isolated from wild-type, *fibulin-4$^{+/-}$*, and *fibulin-4$^{-/-}$* mice at postnatal day 1 (P1). Either a 5′ or 3′ primer set corresponding to mouse *fibulin-4* cDNA sequence was used in the PCRs. The 5′ primer set (5′-GGCCAGATCTATGCTCCCTTT TGCCTCCTG-3′ and 5′-ACATCCACACAGCTCTCCTG-3′) generates a 381-bp fragment, and the 3′ primer set (5′-TGTCGAGAGCAGCCTTCA TC-3′ and 5′-GGCCGTCGACTCAGAAGGTATAGGCTCCCAC-3′) generates a 357-bp fragment. *fibulin-3* primers were used in the positive control.

Morphological and histological analyses. Timed pregnant mice were sacrificed by CO_2 asphyxiation for collection of embryos at E9.5 to E18.5. P1 pups were

sacrificed by cervical dislocation. Sacrificed embryos or P1 mice were immobilized on agarose plates on their back. The ventral side of the embryos was gently dissected away to expose the aorta and other large arteries. Blood vessels were photographed with a dissecting microscope equipped with a charge-coupled device camera.

For histology, whole embryos and tissues dissected from newborn pups were fixed in Bouin's fixative or 4% paraformaldehyde in 0.1 M phosphate buffer (pH 7.2), dehydrated, and embedded in paraffin. Ten-micrometer sections were stained with hematoxylin and eosin or for elastin using elastin van Gieson stain (Sigma).

Transmission electron microscopy. Dissected tissues were fixed overnight in 3% glutaraldehyde in 0.144 M cacodylate buffer, pH 7.2. One-micrometer sections of plastic-embedded samples were cut and stained with methylene blue to examine the integrity of the tissue. Thin sections were cut on a Reichert Ultracut microtome, counterstained with uranyl acetate, and examined and photographed with a Philips CM-12S electron microscope.

Tissue desmosine assay. Tissue samples from P1 mice were collected from the thoracic aorta and lung. The tissues were hydrolyzed in 6 N HCl at 100°C for 24 h, evaporated to dryness, and redissolved in water. Desmosine was quantified by radioimmunoassay as previously described (49), and hydroxyproline was determined by amino acid analysis.

Northern blot analysis. Eight micrograms of total RNA isolated from various tissues of wild-type, *fibulin-4$^{+/-}$*, and *fibulin-4$^{-/-}$* mice at P1 was separated on a 1% formaldehyde-agarose gel and transferred to a Hybond-XL nylon membrane (Amersham). Prehybridization was performed by incubating the membrane for 4 h at 65°C in the hybridization buffer without the probe. The membrane was hybridized with a ^{32}P-labeled probe using the Megaprime DNA Labeling system (Amersham). The *fibulin-4* probe is a 357-bp mouse *fibulin-4* cDNA fragment amplified by RT-PCR, the tropoelastin probe is a 3.6-kb mouse tropoelastin cDNA fragment containing the entire coding sequence released by SalI/NotI digestion from vector pCMV-SPORT6-mELN (Open Biosystems), and the LOX probe is a 4-kb mouse *Lox* cDNA fragment released by SalI-NotI digestion from vector pCMV-SPORT6-mLOX (Open Biosystems). After the *fibulin-4* probe was used, the same membranes were stripped by being boiled for 30 min in 0.1% sodium dodecyl sulfate (SDS), washed, and hybridized with other probes. A mouse glyceraldehyde-3-phosphate dehydrogenase (GAPDH) probe was used as a control. A 1.2-kb GAPDH fragment was generated by RT-PCR using the primers 5′-CCGCATCTTCTTGTGCAGTGCCA-3′ and 5′-CGAACTTTATTG ATGGTATTCAAGAGA.

Production of MAbs against human fibulin-4. cDNA encoding human fibulin-4 (OriGene Technologies) without signal peptide was cloned into vector pGEX-4T-2 (Pharmacia) to generate fibulin-4 fused with glutathione S-transferase (GST). GST–fibulin-4 or GST was purified as described previously (36). Four mice were immunized with GST–fibulin-4. Sera (polyclonal antibodies) from all the mice were characterized with both GST fusion proteins and lysates of transfected 293T cells expressing recombinant fibulin-4. Hybridomas were derived from one of these mice. Several different clones producing monoclonal antibodies (MAbs) against fibulin-4 were identified by enzyme-linked immunosorbent assay. Clones 7B9 (immunoglobulin G2a [IgG2a]) and 11E2 (IgG2b) are of high specificity and titer.

Transfection, immunoprecipitation, and immunoblotting. 293T cells were transfected with a control plasmid, pCMV6-XL4-fb4 (human *fibulin-4* cDNA), pCMV6-XL6-heln (human *tropoelastin* cDNA obtained from Origene), or both pCMV6-XL4-fb4 and pCMV6-XL6-heln with Lipofectamine (Invitrogen). At 48 h after transfection, cells were lysed. Immunoprecipitation and immunoblotting using antibodies against fibulin-4 and human elastin (Elastin Products Company) were performed as previously described (34) with modifications. To avoid the interference of the IgG heavy chain in interpreting results of immunoblotting following immunoprecipitation by the same or similar antibodies, immunoprecipitation was performed with antibodies covalently coupled to protein A-Sepharose. Anti-fibulin-4 MAb 7B9 or a rabbit anti-human tropoelastin polyclonal antibody (Elastin Products Company) was cross-linked to protein A-Sepharose CL-4B (Pharmacia) using dimethylpimelimidate (Sigma) as previously described (35). For each immunoprecipitation, cell lysate containing 200 μg of total protein was diluted to 1 ml with lysis buffer containing 50 mM Tris (pH 8.0), 150 mM NaCl, 10% glycerol, 0.5% NP-40, 0.5% Triton X-100, 1 mM phenylmethylsulfonyl fluoride, and a 1:100 dilution of protease inhibitor mixture III (Calbiochem). A total of 25 μl of antibody-protein A beads was incubated with the cell lysate for 4 h at 4°C. The immunoprecipitates were washed and resuspended in 30 μl of SDS-polyacrylamide gel electrophoresis (SDS-PAGE) sample buffer; 10 μl of the suspension was loaded to each well, resolved by SDS-PAGE on a 10% gel, and transferred onto a polyvinylidene difluoride membrane (Millipore). Anti-fibulin-4 MAb 11E2 or the anti-human tropoelastin antibody was used in immu-
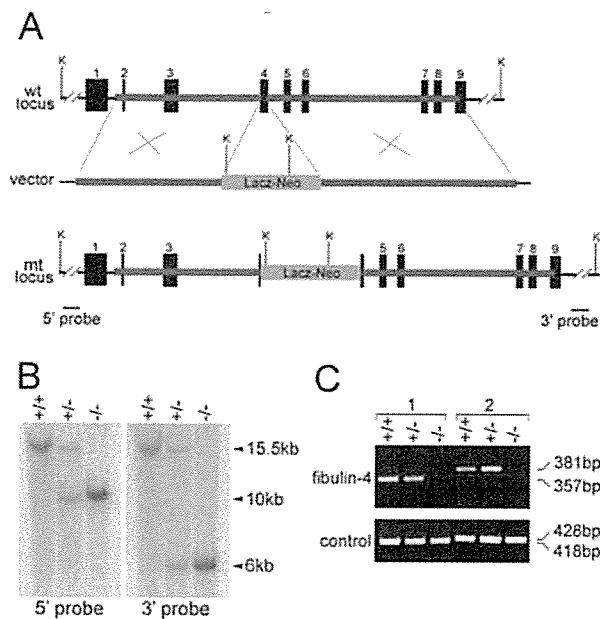
FIG. 1. Targeted disruption of the mouse *fibulin-4* gene. (A) Targeting strategy. Thick lines represent the homology arms used for constructing the targeting vector. Numbered solid boxes depict *fibulin-4* exons. The external 5' and 3' probes (B) are indicated as two bars beneath the mutant (mt) locus. wt, wild-type; K, KpnI. (B) Southern blot analysis of tail genomic DNA from wild-type (+/+), heterozygous (+/−), and homozygous (−/−) mice. The 15.5-kb wild-type band was detected by both 5' and 3' probes, the 10-kb mutant band was detected by the 5' probe, and the 6-kb mutant band was detected by the 3' probe. (C) RT-PCR analysis of mouse RNA. No PCR product was detected for homozygous mice with either a 3' (1) or 5' (2) primer set, indicating the absence of *fibulin-4* mRNA in these mice. In the positive control, PCR products were detected for all mice when a 3' or 5' primer set was used for fibulin-3.

noblotting. Alkaline phosphatase-conjugated anti-mouse IgG2b or anti-rabbit IgG (Jackson ImmunoResearch Laboratories) was used as a secondary antibody.

Production of recombinant fibulin-4 and solid-phase binding assay. Plasmid pEF6/V5 (Invitrogen) was modified to place a preprotrypsin signal sequence, a FLAG tag, and a His_6 tag to the N terminus of its inserted protein. Mouse *fibulin-4* cDNA without the signal sequence was subcloned to the modified vector. 293T cells were transfected with the resulting vector with Lipofectamine Plus (Invitrogen), according to the manufacturer's protocol. Stably transfected cells were selected with Blasticidin (Invitrogen). Recombinant fibulin-4 was purified from the serum-free conditioned medium of stable lines with TALON His-Tag Purification resins (Clontech) according to the manufacturer's instructions. The purity of the protein was confirmed by Coomassie blue staining of a SDS-PAGE gel, and the protein concentration was determined with Coomassie Plus reagent (Pierce). Various concentrations of purified fibulin-4 in Tris-buffered saline containing 2% skim milk with 2 mM $CaCl_2$ or 5 mM EDTA were used as ligands for a solid-phase binding assay. Recombinant bovine tropoelastin was prepared as previously described (26). Solid-phase binding assays using purified tropoelastin were performed as previously described (54) with the modification of 2 mM $CaCl_2$ or 10 mM EDTA added in the buffer. Anti-FLAG M2 antibody (Sigma) (1:2,000) was used as a primary antibody; horseradish peroxidase-conjugated anti-mouse IgG antibody (Santa Cruz) (1:3,000) was used as a secondary antibody. A color reaction assay was performed with the R&D Substrate Reagent Pack, followed by optic density measurement at 450 nm.

Cell culture and immunostaining. Normal human skin fibroblasts were cultured in Dulbecco's modified Eagle's medium with 10% fetal bovine serum at a density of 8 × 10⁴ cells per 1 well of 24-well plate (day 0). On day 3, the medium was changed to Dulbecco's modified Eagle's medium-F12 with 10% fetal bovine serum and recombinant mouse fibulin-4 at a concentration of 5 μg/ml. On day 12, cells were fixed with 100% methanol and stained with rabbit antielastin antibody PR533 (1/100; Elastin Products Company) and mouse anti-FLAG M2 antibody

(1/100; Sigma). Alexa Fluor 546-conjugated anti-rabbit IgG (1/100; Invitrogen) and Alexa Fluor 488-conjugated anti-mouse IgG (1/100; Invitrogen) were used as secondary antibodies. Stained cells were mounted with Vectashield with 4,6-diamino-2-phenylindole (DAPI) (Vector) and examined with a confocal microscope (Carl Zeiss).

RESULTS

Targeted inactivation of the *fibulin-4* gene results in perinatal lethality. The mouse *fibulin-4* gene was inactivated by insertion of a promoterless *lacZ* and a neomycin-resistant gene cassette into exon 4 (Fig. 1A). Homologous recombinants were identified by Southern blot analysis (Fig. 1B). The absence of *fibulin-4* mRNA was confirmed by RT-PCR (Fig. 1C) and Northern blot analysis (see Fig. 7). We found no adult homozygous offspring of *fibulin-4*$^{+/−}$ crossings, raising the possibility that ablation of fibulin-4 causes early lethality. Genotype analysis of offspring at several developmental stages indicated that the number of wild-type, heterozygous, and homozygous animals were distributed in a normal Mendelian pattern at embryonic stages E11.5 and E18.5 (Table 1). However, most *fibulin-4*$^{−/−}$ mice died during birth, only 10% survived to P1, and all the homozygous mice died by P2 (Table 1). The frequency of heterozygous animals was about twice that of the wild type and thus was not affected by the disruption of one *fibulin-4* allele. These results demonstrate that lack of fibulin-4 causes perinatal lethality in mice.

Severe vascular and lung defects in *fibulin-4*$^{−/−}$ mice. The gross appearances of wild-type, *fibulin-4*$^{+/−}$, and *fibulin-4*$^{−/−}$ mice at P1 were similar. However, on dissection, *fibulin-4*$^{−/−}$ mice exhibited severe vascular and lung defects. The arteries were tortuous, with irregularities including narrowing, dilatation, aneurysms, rupture, and resulting hemorrhages. The abnormalities were most severe in the aorta (Fig. 2B) and large arteries but occurred in other arteries as well. In addition, all live-born *fibulin-4*$^{−/−}$ mice were found to have expanded lungs. Histological examinations showed markedly enlarged distal airspaces, similar to those of emphysematous lungs (Fig. 2D). No obvious difference was observed in other organs. Despite the severe phenotype exhibited by homozygous animals, heterozygous (*fibulin-4*$^{+/−}$) mice are fertile, have a normal life span, and appear to be indistinguishable from the wild-type littermates.

The earliest abnormality appears in *fibulin-4*$^{−/−}$ embryos at E12.5. To determine the onset time of defects in *fibulin-4*$^{−/−}$ mice, we studied different developmental stages of the mice. The earliest abnormality noted was a uniformly narrowing of the descending aorta in *fibulin-4*$^{−/−}$ embryos at E12.5 (Fig. 3B). The outer diameter of the aorta in *fibulin-4*$^{−/−}$ mice was only

TABLE 1. Genotype frequency of offspring from *fibulin-4*$^{+/−}$ mouse breedings

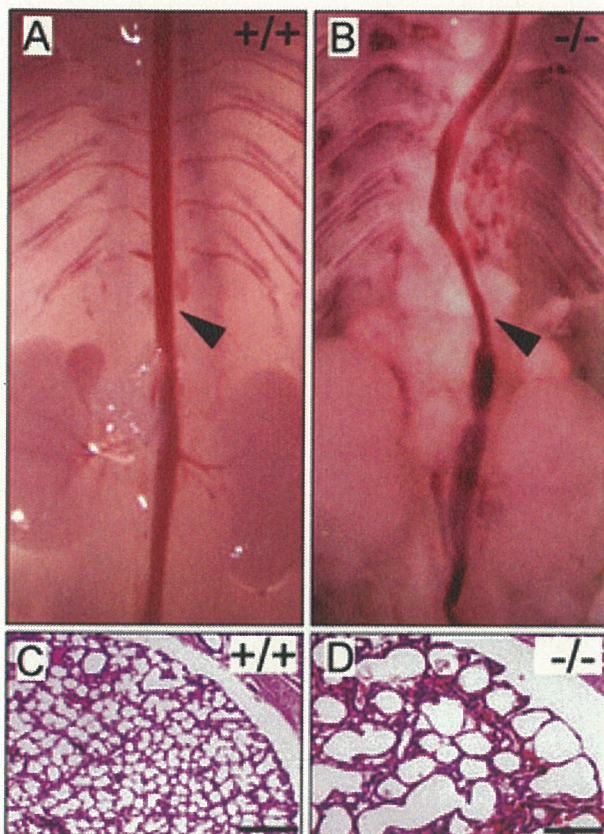| Stage	No. of animals (%) of genotype:			Total no.
	+/+	+/−	−/−	
E11.5	16 (31)	23 (45)	12 (24)	51
E18.5	18 (21)	45 (52)	23 (27)	86
P1	33 (32)	61 (59)	10 (10)	104
P2	46 (32)	97 (67)	1 (<1)	144
P3	53 (31)	118 (69)	0	171

FIG. 2. Aorta and lung defects in *fibulin-4⁻/⁻* mice. (A and B) Aorta (arrowheads) of *fibulin-4⁺/⁺* and *fibulin-4⁻/⁻* mice at P1. (C and D) Hematoxylin and eosin staining of lung sections from mice at P1. The airspaces are significantly enlarged in *fibulin-4⁻/⁻* mice. Scale bars, 400 μm.

FIG. 3. The earliest abnormality in *fibulin-4⁻/⁻* mice at E12.5. (A and B) Aortas of *fibulin-4⁺/⁺* and *fibulin-4⁻/⁻* embryos at E12.5. (C to F) Hematoxylin and eosin staining of cross sections of descending aorta from E12.5 embryos. Note the smaller diameter and thicker wall of the *fibulin-4⁻/⁻* aorta (D). In contrast to the elongated, spindle-shaped cells (E, arrow) in wild-type mice, aortic wall cells were round in the *fibulin-4⁻/⁻* mice (F, arrow). Scale bars, 50 μm (C and D) and 20 μm (E and F).

one-half to two-thirds that of wild-type littermates. Histological analyses of cross sections showed that the aortic walls of *fibulin-4⁻/⁻* mice were nearly twice as thick as those of wild-type mice (Fig. 3D). However, the thickening of the *fibulin-4⁻/⁻* aortic wall did not appear to be the result of subendothelial overproliferation of cells, as the number of cells was similar in both *fibulin-4⁻/⁻* and wild-type aortic wall cross sections. There were 193 ± 3 cells for the wild type (data represent means and standard deviations for results with four mice) and 188 ± 7 cells for the homozygote (four mice) in a cross section of the aortic wall at a similar level of the thoracic aorta as shown in Fig. 3C and D. In contrast to the elongated and spindle-shaped cells in wild-type mice (Fig. 3E), the *fibulin-4⁻/⁻* aortic smooth muscle cells were round and appeared to be less stretched (Fig. 3F). The narrowing and the cell shape difference of the *fibulin-4⁻/⁻* aorta became less obvious at E13.5 and at older embryonic ages, likely due to passive expansion of the aorta caused by the dramatic increase in systemic blood pressure during these stages (22). Aortic tortuosity and irregularity were noticeable at E15.5 and became more pronounced with age in homozygous animals. These aorta abnormalities were not observed in *fibulin-4⁺/⁻* embryos.
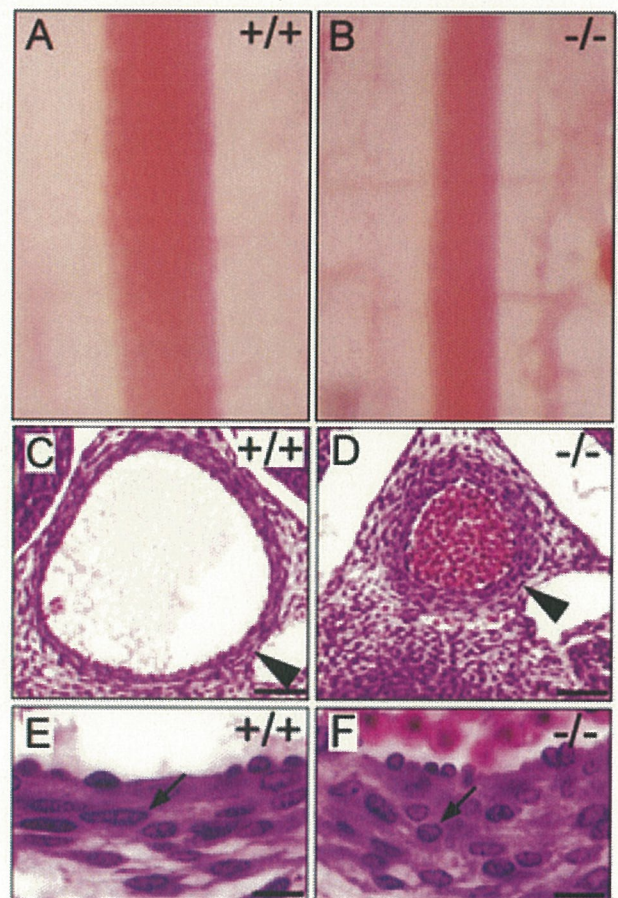
fibulin-4⁻/⁻ mice do not form elastic fibers. The vascular and lung abnormalities of *fibulin-4⁻/⁻* mice were suggestive of elastic fiber defects. The appearance of abnormalities, coincident with the onset of elastogenesis in mice, suggests that genesis of elastic fibers may be impaired in *fibulin-4⁻/⁻* mice. Thus, we stained tissue sections from E12.5 to P1 with elastin van Gieson staining, which specifically stains elastic fibers. In the wild type, the innermost elastic lamina of the aorta was identifiable at E13.5 under a light microscope (Fig. 4A). By E14.5, four elastic laminae could be distinguished (Fig. 4C). All five elastic laminae were present at E16.5 or older ages (Fig. 4E and G). In contrast, no continuous elastic lamina was observed in the *fibulin-4⁻/⁻* aorta at any stage (Fig. 4B, D, F, and H). Instead, irregular elastin aggregates were visible at E14.5 (Fig. 4D), and more and larger aggregates accumulated with age (Fig. 4F and H). In the lung and skin, elastic fibers were not distinguishable by light microscopy at any embryonic stages. At P1, fine elastic fibers could be observed in lung and the hypodermal connective tissue of the skin of wild-type mice (Fig. 5A and C) but not in *fibulin-4⁻/⁻* mice (Fig. 5B and D). Despite this, the skin of *fibulin-4⁻/⁻* mice did not show obvious
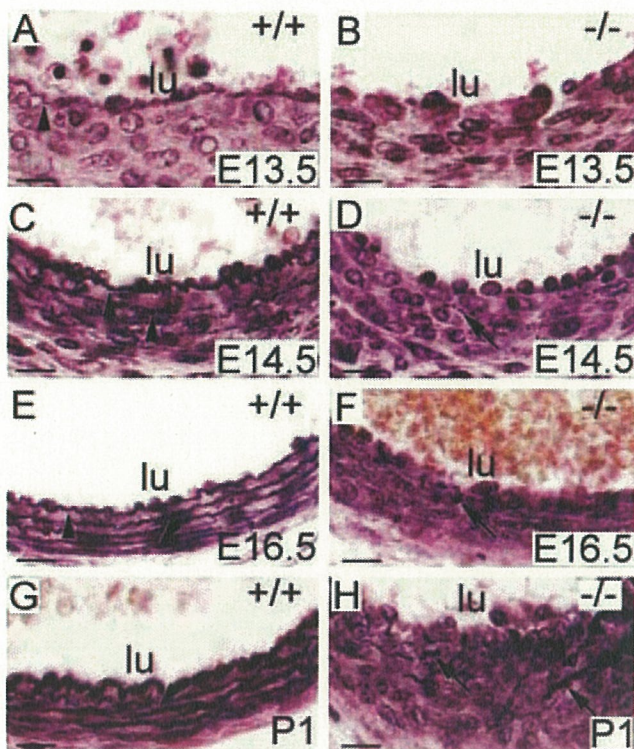
FIG. 4. Lack of elastic lamina in the *fibulin-4⁻/⁻* aorta. Elastin van Gieson staining of cross sections of descending aortae at different developmental stages is shown. The innermost elastic lamina (arrowheads) was identifiable in the wild-type aorta at E13.5 (A) and became more numerous and thicker at subsequent developing stages (C, E, and G). Only irregular elastin aggregates (arrows) were observed in the *fibulin-4⁻/⁻* aorta (B, D, F, and H). lu, lumen. Scale bars, 20 μm.
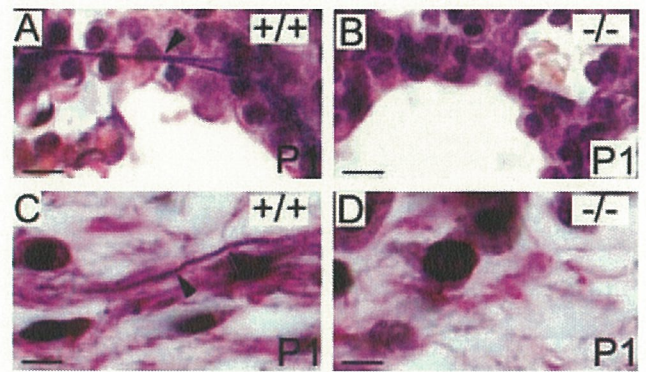

FIG. 5. Lack of elastic fibers in the skin and lung of *fibulin-4⁻/⁻* mice. (A and B) Elastin van Gieson staining of lung sections from P1 mice. Fine branched elastic fibers (arrowhead) were present in the wild-type (A) but not *fibulin-4⁻/⁻* (B) lung. (C and D) Elastin staining of skin sections from P1 mice. Elastic fibers were observed in the hypodermal connective tissue area of the wild-type skin (C, arrowhead) but not in the *fibulin-4⁻/⁻* skin (D). Scale bars, 10 μm (A and B) and 5 μm (C and D).

gross differences at this young age. Elastic fibers of *fibulin-4⁺/⁻* mice were similar to those of wild-type littermates. These results indicate that fibulin-4 is required for general elastogenesis.

Elastin aggregates containing electron dense rod-like filaments in *fibulin-4⁻/⁻* mice. To further understand the elastic fiber defects in *fibulin-4⁻/⁻* mice, we examined the aortae of E14.5 and P1 mice by electron microscopy (Fig. 6). Consistent with the finding by light microscopy, no intact elastic lamina was observed in the *fibulin-4⁻/⁻* aorta at either E14.5 or P1. Continuous elastic lamina was present in the wild-type aorta (Fig. 6A and C), but only irregular elastin aggregates were found in the *fibulin-4⁻/⁻* aorta at both stages (Fig. 6B and D, arrows). Noticeably, the content of the elastin aggregates appeared to be different from that of normal elastic fibers. Instead of an amorphous content, these elastin aggregates contained distinguishable electron-dense substances. Under higher magnification, dark rod-like filaments with similar sizes were seen to be evenly distributed in the elastin aggregates (Fig. 6F). These findings demonstrate that elastin does not properly assemble without fibulin-4.

Desmosine content is severely reduced in *fibulin-4⁻/⁻* mice. To determine whether mature elastin content is affected in *fibulin-4⁻/⁻* mice, we assessed the level of desmosine, an elastin cross-link-specific amino acid, in the aorta and lungs of

wild-type, heterozygous, and homozygous mutant mice. As shown in Table 2, elastin cross-linking was nearly absent in *fibulin-4⁻/⁻* mice. There was a 94% decrease in the amount of desmosine in the aorta and 88% decrease in lungs of *fibulin-4⁻/⁻* mice compared with wild-type mice. Interestingly, there was a near 20% increase in the amount of desmosine in heterozygous mutants compared with wild-type mice (Table 2), although this difference was not statistically significant ($P > 0.05$ in a t test). We did not find any difference in the level of hydroxyproline, an indicator of collagen content, between wild-type and *fibulin-4⁻/⁻* mice (data not shown), indicating that the amount of collagen did not differ in *fibulin-4⁻/⁻* mice.

Tropoelastin and LOX expression is not affected in *fibulin-4⁻/⁻* mice. Elastin cross-linking is catalyzed by LOX family enzymes. Among the five known members, LOX has been shown to be necessary for elastic fiber development (20, 31). To determine whether lack of fibulin-4 causes elastinopathy by affecting tropoelastin or *Lox* expression, we examined the mRNA levels of *fibulin-4*, tropoelastin, and *Lox* in wild-type, heterozygous, and homozygous littermates at P1. As shown in Fig. 7, while heterozygotes showed reduced *fibulin-4* mRNA levels compared to those in wild-type mice and homozygotes had no detectable *fibulin-4* mRNA, all of them had similar levels of tropoelastin or *Lox* expression. Elastin has been shown to have an antiproliferative effect on vascular smooth muscle cells, and mice lacking elastin (*ELN⁻/⁻*) die of vascular occlusion resulting from subendothelial cell proliferation (27). The unaffected tropoelastin expression is consistent with the lack of cell overproliferation and the accumulation of irregular elastin aggregates in *fibulin-4⁻/⁻* mice.

Fibulin-4 interacts with tropoelastin and assembles into elastic fibers. To investigate possible mechanisms by which fibulin-4 affects elastogenesis, we assessed the potential for interaction between fibulin-4 and elastin. Recombinant mouse fibulin-4 was expressed and purified from stably transfected 293T cell medium (Fig. 8A). A FLAG tag and a His₆ tag were added at the N terminus of fibulin-4 without its signal peptide to facilitate the purification and characterization of fibulin-4.
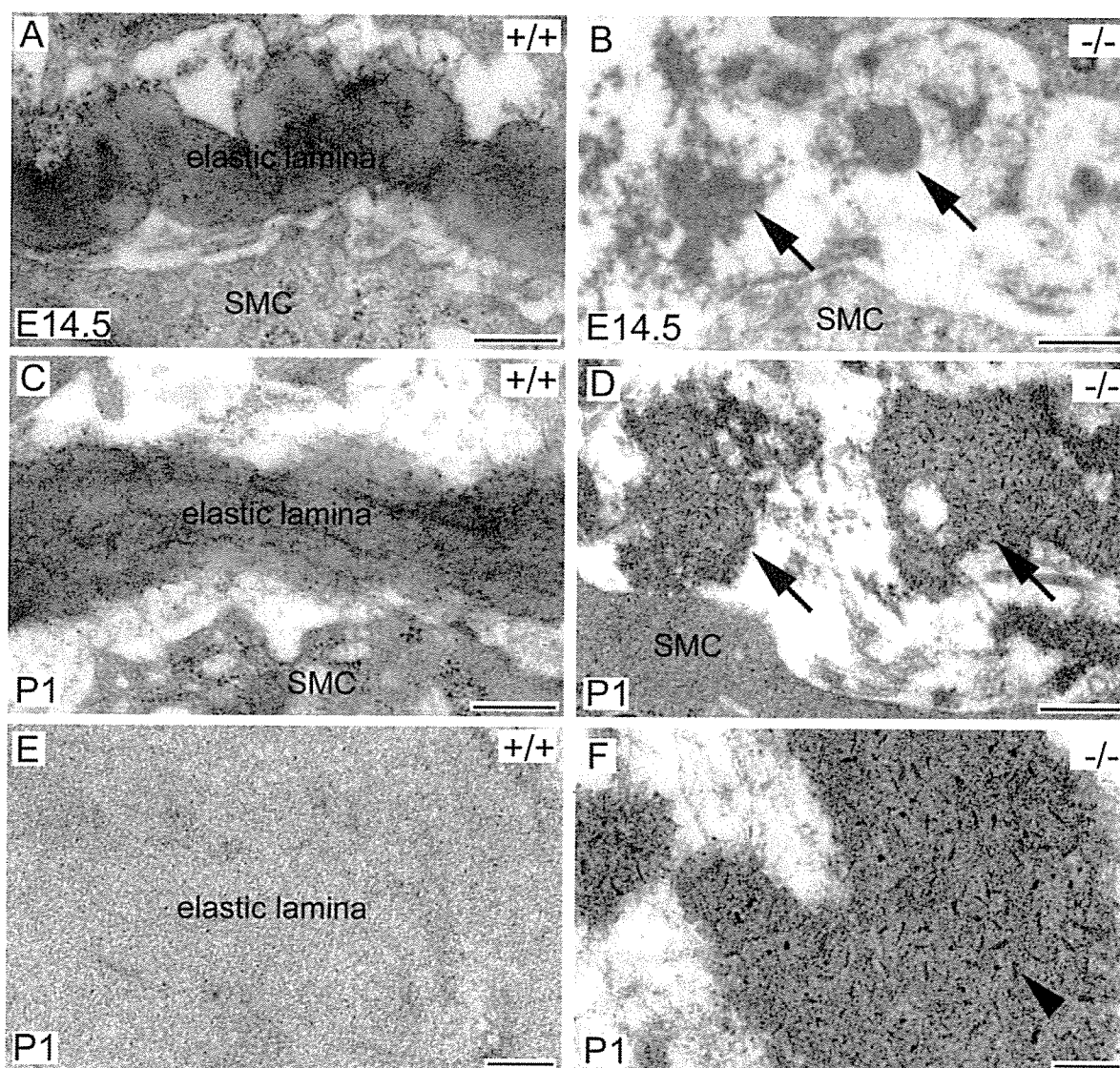
FIG. 6. Electron microscopy of elastic laminae in *fibulin-4*$^{-/-}$ mice. (A to D) Descending aorta cross sections from E14.5 (A and B) and P1 (C and D) mice. The wild-type aorta contained continuous elastic lamina (A and C). In contrast, irregular elastin aggregates (arrows) were randomly distributed in the *fibulin-4*$^{-/-}$ aorta (B and D). Under higher magnification (E and F), the wild-type elastic lamina appeared to be amorphous (E). But distinct, dark rod-like filaments (F, arrowhead) were evenly distributed in the *fibulin-4*$^{-/-}$ elastin aggregates. SMC, smooth muscle cell. Scale bars, 400 nm (A to D) and 100 nm (E and F).

The tagged protein was secreted from a preprotrypsin signal sequence. Although we found that untagged fibulin-4 was secreted efficiently from its native signal peptide, the C-terminal-tagged fibulin-4 was poorly secreted. It is possible that the

TABLE 2. Desmosine in picomoles per milligram of protein in aorta and lung at P1

Genotype (n)	Desmosine ± SD (% of wild type) in:	
	Aorta	Lung
+/+ (12)	419.05 ± 125.94 (100)	29.7 ± 14.87 (100)
+/− (21)	501.86 ± 133.85 (120)[a]	35.63 ± 9.08 (120)[b]
−/− (6)	25.35 ± 8.69 (6)[c]	3.15 ± 1.45 (12)[c]

[a] $P = 0.09$, compared to the wild type by t test.
[b] $P = 0.23$, compared to the wild type by t test.
[c] $P < 0.0001$, compared to the wild type by t test.

C-terminal domain affects protein folding and is sensitive to modification. In a solid-phase binding assay, purified tropoelastin was used as an immobilized protein substrate, and fibulin-4 was used as a soluble ligand. As shown in Fig. 8B, fibulin-4 bound strongly to tropoelastin in the presence of Ca^{2+} and the binding was inhibited in the presence of EDTA, suggesting that calcium is required for the binding and the calcium-binding epidermal growth factor domains of fibulin-4 may be necessary for this binding. However, it has not been demonstrated experimentally that fibulin-4 binds calcium. No binding was observed between fibulin-4 and a control substrate (bovine serum albumin). These results indicate that fibulin-4 and tropoelastin can interact directly.

To assess whether fibulin-4 and tropoelastin interact in solution, we performed a coimmunoprecipitation assay. Human *fibulin-4* cDNA, human *tropoelastin* cDNA, or both were trans-